Available online at www.sciencedirect.com
SCIENCE DIRECT®
ELSEVIER
Nuclear Instruments and Methods in Physics Research B 234 (2005) 387–411
NIM B
Beam Interactions with Materials & Atoms
www.elsevier.com/locate/nimb

Evaluation of ^{4}He production cross-section for tantalum, tungsten and gold irradiated with neutrons and protons at the energies up to 1 GeV

C.H.M. Broeders, A.Yu. Konobeyev *

Institut für Reaktorsicherheit, Forschungszentrum Karlsruhe GmbH, P.O. Box 3640, 76021 Karlsruhe, Germany

Received 25 November 2004; received in revised form 7 February 2005
Available online 31 May 2005

Abstract

Popular nuclear models and approaches used for the description of the α-particle emission in the nucleon induced reactions at the intermediate energies were analyzed. The α-particle emission spectra, the non-equilibrium α-particle yields and the total α-production cross-sections were calculated with the help of the GNASH code, the modified ALICE code, the DISCA code and the different codes from the MCNPX package. The results of the calculation were compared with available experimental data, systematics values and data from ENDF/B-VI and JENDL-HE. Data from FENDL/A-2, JENDL-3.3, CENDL-2 and JEFF-3/A were also used for the comparison with calculations and measured data for neutron induced reactions below 20 MeV. The discrepancies between the calculations and the experimental data have been analyzed. The α-particle production cross-section has been evaluated for ^{181}Ta, ^{nat}W and ^{197}Au at the energies of the incident neutrons and protons from several MeV to 1 GeV.

PACS: 25.45.−z; 25.60.Dz; 27.50.+e90; 20.25.Rm

Keywords: Tantalum; Tungsten; Gold; Helium production; Cross-section; Intermediate energies; Protons; Neutrons

1. Introduction

The study of helium production in nuclear reactions is an important part of the research of radiation damage of materials. Recently the determination of reliable helium production cross-sections for tantalum and tungsten has got a special interest for the TRIGA/TRADE project [1]. Tantalum and tungsten are proposed as materials of the target, which undergone the intense influence of the primary proton beam and secondary neutrons produced in nuclear reactions.

* Corresponding author. Tel.: +49 7247 82 2638; fax: +49 7247 82 3718.
E-mail address: konobeev@irs.fzk.de (A.Yu. Konobeyev).

0168-583X/$ - see front matter © 2005 Elsevier B.V. All rights reserved.
doi:10.1016/j.nimb.2005.02.029

The available experimental data for helium production in tantalum and tungsten irradiated with nucleons are not enough for detail testing of the methods of the calculation and the determination of the nuclear model parameters relevant to the helium isotope emission at the energies of the primary particles up to 1 GeV. A considerable amount of the experimental data for ^{4}He production including the total yields and α-particle emission spectra is available for ^{197}Au. These data are used in the present work for testing of theoretical models.

The goal of this work is the study and the evaluation of the ^{4}He-production cross-section for ^{181}Ta, W and ^{197}Au irradiated with neutrons and protons at low and intermediate energies.

The evaluation of the cross-sections was done at the energies from several MeV up to 1 GeV. The evaluation included the analysis of available experimental data and the contents of evaluated data libraries (ENDF/B-VI, JENDL-HE, JENDL-3.3, CENDL-2, FENDL/A-2, JEFF-3/A), the calculations with the help of the modern theoretical approaches, codes and systematics. The brief description and the analysis of the models used for the cross-section calculation are given in Section 2. Section 3 presents the comparison of the results of calculations with experimental data. The evaluation of the ^{4}He-production cross-section for ^{181}Ta, W and ^{197}Au is discussed in Section 4.

2. Brief description of models and codes used for helium production cross-section calculation

This section describes briefly nuclear models, approaches and codes used in the present work for the calculation of the total and differential ^{4}He-production cross-sections for nucleon induced reactions.

2.1. Pre-compound model combined with evaporation model

2.1.1. The GNASH code

The GNASH code implements the pre-equilibrium exciton model and the statistical Hauser–Feshbach model [2]. The basic description of the code and the models used is given in [3].

The pre-equilibrium nucleon emission is described by the following expression resulting from an analytical solution of master equations of the exciton model:

$$\frac{\mathrm{d}\sigma}{\mathrm{d}\varepsilon_\mathrm{x}} = \sigma_\mathrm{non}(E_\mathrm{p})\frac{(2S_\mathrm{x}+1)\mu_\mathrm{x}\varepsilon_\mathrm{x}\sigma_\mathrm{x}^\mathrm{inv}(\varepsilon_\mathrm{x})}{\pi^2\hbar^3} \times \sum_{n=n_0} R_\mathrm{x}(n)\frac{\omega(p-1,h,U)}{\omega(p,h,E)}\frac{1}{\lambda_n^+ + \lambda_n^- + \gamma_n}D(n), \quad (1)$$

where σ_non is the cross-section of non-elastic interaction of the primary particle with a nucleus at the kinetic energy E_p; S_x and μ_x are spin and reduced mass of the outgoing nucleon of x-type; ε_x is the kinetic energy of the nucleon; $\sigma_\mathrm{x}^\mathrm{inv}$ is the inverse reaction cross-section for x-particle; $\omega(p,h,E)$ is the density of exciton states with "p" particles and "h" holes ($p+h=n$) at the excitation energy E calculated according to Williams [4]; U is the final excitation energy, $U = E - Q_\mathrm{x} - \varepsilon_\mathrm{x}$ and Q_x is the separation energy for nucleon; λ_n^+ and λ_n^- are transition rates from the n-exciton state to the states with $n+2$ and $n-2$ excitons, correspondingly; γ_n is the nucleon emission rate; $R_\mathrm{x}(n)$ is the factor describing the difference between the number of neutrons and protons in the n-exciton state; $D(n)$ is the factor, which takes into account the "depletion" of the n-exciton state due to the nucleon emission; n_0 is the initial exciton number. The transition rates λ_n^+ and λ_n^- are calculated as follows:

$$\lambda_n^\pm = (2\pi/\hbar)\langle|M|^2\rangle\omega^\pm(n,E), \quad (2)$$

where $\langle|M|^2\rangle$ is the averaged squared matrix element for two-body interaction parameterized as the set of functions of E/n in [5]; $\omega^\pm$ is the density of states available for transitions from "n" to "$n+2$" and "$n-2$" exciton states calculated according to [3,6].

The multiple pre-equilibrium emission (two precompound nucleons escape) is described according to [7]. The improvement of the approach [7] is discussed in [8].

The pre-equilibrium α-particle emission spectrum for nucleon induced reaction is calculated as a sum of components corresponding to the mechanism of pick-up and knock-out

$$\frac{d\sigma}{d\varepsilon_\alpha} = \frac{d\sigma^{\text{pick-up}}}{d\varepsilon_\alpha} + \frac{d\sigma^{\text{knock-out}}}{d\varepsilon_\alpha}, \quad (3)$$

and the components are evaluated according to the phenomenological Kalbach approach [6]

$$\frac{d\sigma^{\text{pick-up}}}{d\varepsilon_\alpha} = (2S_\alpha + 1)A_\alpha \varepsilon_\alpha \sigma_\alpha^{\text{inv}}(\varepsilon_\alpha)\omega_f^{\text{pick-up}}(U) \times f(N,Z,\Delta_\nu,\Delta_\pi)(780/A)^3 E_p^{-6} 2.8 \times 10^{-3}, \quad (4)$$

where S_α and A_α are spin and mass number of the α-particle emitted; A, Z, N are atomic mass number, atomic number and number of neutrons for a target nuclide, respectively; the energy units are MeV; $\omega_f^{\text{pick-up}}$ is the final state density for pick-up process and "f" is the function defined below:

$$\omega_f^{\text{pick-up}} = \frac{6}{\Delta_\nu \Delta_\pi} \sum_{i=1}^{3} \omega(0,i,U), \quad (5)$$

$$f(N,Z,\Delta_\nu,\Delta_\pi) = (2Z/A)^{6\Delta_\pi}(2N/A)^{(1-\Delta_\pi)\Delta_\nu(\Delta_\nu+1)/2}, \quad (6)$$

where Δ_ν and Δ_π are number of neutrons and protons transferred in the pick-up process. The knock-out component of spectrum is calculated as follows:

$$\frac{d\sigma^{\text{knock-out}}}{d\varepsilon_\alpha} = \sigma_{\text{non}}(E_p) \times \left(\frac{A+1}{AE}\right)^3 (2S_\alpha + 1)A_\alpha \varepsilon_\alpha \sigma_\alpha^{\text{inv}}(\varepsilon_\alpha) \times \omega_f^{\text{knock-out}}(U) f(N,Z,\Delta_\nu,\Delta_\pi) A^{-3} Z 0.06, \quad (7)$$

where the units are mb for the cross-sections and MeV for the energy, $\omega_f^{\text{knock-out}}$ is the final state density for the knock-out process

$$\omega_f^{\text{knock-out}} = g_x g_\alpha \left(U - \frac{1}{2g_x} - \frac{1}{2g_\alpha}\right), \quad (8)$$

here g_x is the single particle density for neutrons and protons depending from projectile, $g_n = N/13$, $g_p = N/13$; the level density for α-particle g_α is equal to $A/52$.

The pre-equilibrium emission of α-particles following the nucleon emission, i.e. the multiple pre-compound α-emission is not considered in the GNASH code.

Equilibrium particle emission is described with the help of the Hauser–Feshbach model. The combination of the exciton model formulated without the consideration of angular momentum (Eq. (1)) and the angular dependent statistical model is discussed in [3,9].

In the present work two different approaches were used for the nuclear level density calculation in equilibrium states. The calculation was done with the help of the Fermi gas model with the nuclear level density parameter depending from the excitation energy [10] and the generalized superfluid model [11].

In the approach of Ignatyuk and coauthors [10] the nuclear level density is described by expressions basing on the Fermi gas model. The nuclear level density parameter is calculated as follows:

$$a(U) = \tilde{a}(1 + \varphi(U)\delta W/U), \quad (9)$$

where U is the energy of the excitation corrected for the odd–even difference in the nuclear level density; $\tilde{a}$ is the asymptotic value of the nuclear level density parameter; δW is the shell correction to the mass formula equal to the difference between experimental mass defect and one calculated from the liquid drop model; $\varphi(U)$ is the dimensionless function equal to

$$\varphi(U) = 1 - \exp(-\gamma U) \quad (10)$$

with $\gamma = 0.054\ \text{MeV}^{-1}$. The asymptotic value $\tilde{a}$ is defined by the equation

$$\tilde{a}/A = \alpha + \beta A, \quad (11)$$

where α and β are parameters defined in [2,11] $\alpha = 0.1375$ and $\beta = -8.36 \times 10^{-5}$, which values are different from ones obtained in the original work [10]. This model is used for the calculation of the nuclear level density at high excitation energy. At low energy of excitation the constant temperature approach [3] is applied for the calculations.

Other model used for the nuclear level density calculation is the generalized superfluid model with the parameters fitted to the cumulative number of low-lying levels and observed neutron resonance densities [11]. The expression for nuclear level density is written as follows:

$$\rho(U,J,\pi) = \rho_{qp}(U',J,\pi)K_{vib}(U')K_{rot}(U'), \quad (12)$$

where $\rho_{qp}(U', J, \pi)$ is the density of quasi-particle nuclear excitation [11], $K_{vib}(U')$ and $K_{rot}(U')$ are the vibrational and rotational enhancement factors at the effective energy of excitation U' calculated according to [11,13].

The nuclear level density parameters are calculated according to the expression [11,12]

$$a(U) = \begin{cases} \tilde{a}(1+\delta W\varphi(U'-E_{cond})/(U'-E_{cond})), & U' > U_{cr}, \\ a(U_{cr}), & U' \leqslant U_{cr}, \end{cases} \quad (13)$$

where the effective energy of excitation U', the critical energy of the phase transition U_{cr} and the condensation energy E_{cond} are calculated according to [11,12]. The function $\varphi(U)$ is defined by Eq. (10) with the γ value equal to $0.4/A^{1/3}$ MeV^{-1}. The asymptotic value of the nuclear level density parameter is equal to

$$\tilde{a}/A = \alpha + \beta A^{-1/3}, \quad (14)$$

where α and β are coefficients obtained in [14] from the fitting of Eq. (14) to the RIPL-1 data [15], $\alpha = 0.118$ and $\beta = -0.172$.

The calculation of the nuclear level density with the help of the Fermi gas model [10] was carried out by the GNASH built-in routines. The constant temperature and Fermi gas expressions for the level density were matched approximately, which corresponds to the input parameter IBSF controlling the level density option equal to 2. The generalized superfluid model [11,12] is used in modified version of the GNASH code [8,14,16].

The neutron and proton optical potential from [17] was used for the calculation of the reaction cross-section and transmission coefficients. The transmission coefficients for α-particles were obtained with the help of the optical potential from [18]. The calculations were carried out by the ECIS96 code [19].

2.1.2. The ALICE/ASH code

The code is based on the geometry dependent hybrid pre-compound decay model [20,21] (GDH) and the evaporation Weisskopf–Ewing model [22]. The ALICE/ASH code is an advanced version of the original M.Blann code [23]. Partly, the modification is described in [24,25]. It concerns the implementation in the code the models describing the pre-compound composite particle emission [26–28] and fast γ-emission [29], different approaches for the nuclear level density calculation [24,25,30] and the model for the fission fragment yield calculation [31,14].

The code under different names [24,25] was successfully used for the preparation of activation data libraries at intermediate energies MENDL [32,30,33], IEAF [34–36] and WIND [37–39,35]. The neutron, charged particle, photon and recoil spectra applied for the composition of nuclear data files, the transport and heat deposition calculations [40,41,35] have been obtained with the help of the code. ALICE/ASH has been used for the description of the heavy cluster pre-compound emission [42] and for the calculation of fission fragment distributions for actinides irradiated with nucleons at intermediate energies [8,14,16].

In the GDH model the pre-equilibrium spectrum of nucleons is calculated as follows [21]:

$$\frac{d\sigma}{d\varepsilon_x} = \pi\lambda^2 \sum_{l=0}^{\infty}(2l+1)T_l \sum_{n=n_0} R_x(n)\frac{\omega(p-1,h,U)}{\omega(p,h,E)} \times \frac{\lambda_x^e}{\lambda_x^e+\lambda_x^+} gD(n), \quad (15)$$

where λ is the reduced de Broglie wavelength of the incident particle; T_l is the transmission coefficient for lth partial wave; $R_x(N)$ is the number of nucleons of x-type in the n-exciton state calculated according to [21]; g is the single particle level density equal to $A/14$; λ_x^e is the emission rate of nucleon calculated with the following formula:

$$\lambda_x^e = \frac{(2S_x+1)\mu_x\varepsilon_x\sigma_x^{inv}(\varepsilon_x)}{\pi^2\hbar^3 g_x}, \quad (16)$$

where the single particle density g_x is equal to $Z/14$ for protons and $N/14$ for neutrons. The intranuclear transition rate λ_x^+ is defined as follows:

$$\lambda_x^+ = V\sigma_0(\varepsilon_x)\rho_l, \quad (17)$$

where V is the velocity of nucleon inside the nucleus; σ_0 is the nucleon–nucleon scattering cross-section corrected for the Pauli principle; ρ_l is the

average nuclear density at the distance from $l\,\lambda$ to $(l+1)\,\lambda$.

For the initial nuclear state with three excitons the density of the excited states $\omega(p, h, E)$ is calculated by the model [43] considering the final depth of the nuclear potential well. The multiple pre-compound emission is described by the approximate approach [21]. As in the GNASH code, only two fast particles escape is considered. The correction made for the high energy tails of (p, x)n and (n, x)p reaction spectra calculated by the GDH model is discussed in [35].

The pre-equilibrium α-particle emission spectrum is calculated as a sum of components corresponding to the mechanism of pick-up and knock-out, Eq. (3). The models used here are rather different from ones implemented in the GNASH code. The contribution of the pick-up mechanism is calculated with the help of the coalescence pick-up model [44,45] combined with the hybrid exciton model [26]

$$\frac{\mathrm{d}\sigma^{\text{pick-up}}}{\mathrm{d}\varepsilon_\alpha} = \sigma_{\text{non}}(E_\text{p}) \sum_{n=n_0} \sum_{k+m=4} F_{k,m}(\varepsilon_\alpha) \times \frac{\omega(p-k,h,U)}{\omega(p,h,E)} \times \frac{\lambda^\text{e}_\alpha(\varepsilon_\alpha)}{\lambda^\text{e}_\alpha(\varepsilon_\alpha)+\lambda^+_\text{x}(\varepsilon_\alpha)} g_\alpha D(n), \tag{18}$$

where $F_{k,m}(\varepsilon_\alpha)$ is the alpha formation factor [44] equal to the probability that the of α-particle is composed of "k" particles above Fermi level and "m" particles below; the residual excitation energy U is equal to $E - Q_\alpha - \varepsilon_\alpha$; λ^e_α is the emission rate of α-particle; λ^+_α is the intranuclear transition rate corresponding to the absorption of α-particle in a nucleus; g_α is the density of single states for α-particle. The emission rate of α-particle is calculated with the following formula:

$$\lambda^\text{e}_\alpha = \frac{(2S_\alpha+1)\mu_\alpha \varepsilon_\alpha \sigma^\text{inv}_\alpha(\varepsilon_\alpha)}{\pi^2\hbar^3 g_\alpha}, \tag{19}$$

and the inverse reaction cross-section for α-particle $\sigma^\text{inv}_\alpha(\varepsilon_\alpha)$ is calculated by the optical model with the parameters described in [23]. The absorption rate of α-particle is defined as follows:

$$\lambda^+_\alpha = 2W^\text{opt}_\alpha/\hbar, \tag{20}$$

where W^opt_α is the imaginary part of the optical potential for α-particle.

The knock-out contribution to the α-particle spectrum is calculated with the following expression [27]:

$$\frac{\mathrm{d}\sigma^{\text{knock-out}}}{\mathrm{d}\varepsilon_\alpha} = \sigma_{\text{non}}(E_\text{p}) \sum_{n=n_0} \varphi_\alpha \frac{g}{g_\alpha p} \times \frac{\omega(p-1,h,U)}{\omega(p,h,E)} \times \frac{\lambda^\text{e}_\alpha(\varepsilon_\alpha)}{\lambda^\text{e}_\alpha(\varepsilon_\alpha)+\lambda^+_\text{x}(\varepsilon_\alpha)} g_\alpha D(n), \tag{21}$$

where the factor $g/(g_\alpha p)$ justifies the substitution of the level density $\omega(\pi, \tilde{\pi}, \nu, \tilde{\nu}, \alpha, \tilde{\alpha}, E)$ for the three-component system (neutron, proton, α-particle) [46,27] by the one-component state density $\omega(p, h, E)$ in Eq. (21); φ_α is the probability of interaction of the incident particle with "pre-formed" α-cluster resulting in its excitation in the nucleus [46].

The pre-compound α-emission after the pre-compound escape of neutrons and protons (multiple pre-equilibrium emission) is taken into account [27]. The formula for the calculation of the pre-compound emission spectrum of α-particle formed due to the nucleon pick-up process and escaped after the pre-equilibrium nucleon emission is written as follows:

$$\frac{\mathrm{d}\sigma}{\mathrm{d}\varepsilon_\alpha} = \pi\lambda^2 \sum_{l=0}^{\infty}(2l+1)T_l \sum_{\text{x}=\pi,\nu}^{2} \int_{E^\text{min}_\text{x}}^{E^\text{max}_\text{x}} \times \sum_{n=n_0} R_\text{x}(n) \frac{\omega(p-1,h,E-Q_\text{x}-\varepsilon_\text{x})}{\omega(p,h,E)} \times \frac{\lambda^\text{e}_\text{x}(\varepsilon_\text{x})}{\lambda^\text{e}_\text{x}(\varepsilon_\text{x})+\lambda^+_\text{x}(\varepsilon_\text{x})} gD(n) \sum_{n'=p+h-1} \times \sum_{k+m=4} F_{k,m}(\varepsilon_\alpha) \times \frac{\omega(p'-k,h',E-Q_\text{x}-\varepsilon_\text{x}-Q'_\alpha-\varepsilon_\alpha)}{\omega(p',h',E-Q_\text{x}-\varepsilon_\text{x})} \times \frac{\lambda^\text{e}_\alpha(\varepsilon_\alpha)}{\lambda^\text{e}_\alpha(\varepsilon_\alpha)+\lambda^+_\text{x}(\varepsilon_\alpha)} g_\alpha D(n')\,\mathrm{d}\varepsilon_\text{x}, \tag{22}$$

where "x" refers to proton and neutron; Q'_α is the separation energy for α-particle in the nucleus formed after the emission of nucleon of x-type;

E_x^{min} and E_x^{max} define the energy range, where the emission of the x-particle occurs. The analogous formula is written for α-particle knock-out process following the fast nucleon emission [27]. The successive emission of three and more pre-equilibrium particles is not considered.

The following parameters of the models were used for the calculations: $\sum_{k+m=4} F_{k,m} = 0.3$ and $\varphi_\alpha = 0.012$. The imaginary part of the optical potential for α-particle was calculated as follows: $W_\alpha^{opt} = (\varepsilon_\alpha/\varepsilon_0)W'$ at $\varepsilon_\alpha \leqslant \varepsilon_0$, $W_\alpha^{opt} = W'$ at $\varepsilon_0 < \varepsilon_\alpha < 72$ MeV, $W_\alpha^{opt} = W' \cdot \exp(0.06\varepsilon_\alpha - 4.32)$ at $\varepsilon_\alpha \geqslant 72$ MeV, where $W' = \beta\ W_0$ and $\varepsilon_0 = 0.228A$, $\beta = 0.25$. The value of W_0 was taken from [47,48] $W_0 = 10 + 0.345(A - 2Z)$ MeV. The values of the parameters listed above are from [24,25] except the W_α^{opt} value calculation at the energy ε_α above 72 MeV. The adopted value of the single state density for α-particle is equal to $A/13$ (see discussion in [25]).

Principally the same models used in the GNASH calculations were applied to the nuclear level density calculation. In a difference with Section 2.1.1, the asymptotic value of the level density parameter in the Fermi gas model [10] was defined with α and β coefficients obtained in the original work [10] $\alpha = 0.154$ and $\beta = -6.3 \times 10^{-5}$. The model [10] was used at the high excitation energy of nuclei. At low excitation energy the constant temperature approach [24] was applied. In the calculations using the superfluid model the systematics values of parameters [12,30,25] were used rather than the individual parameter values [11]. The asymptotic value of nuclear level density parameter was calculated as follows [12,30,25]: $\tilde{a}/A = 0.073 + 0.115A^{-1/3}$.

2.2. Intranuclear cascade evaporation model describing cascade α-cluster emission

2.2.1. The DISCA-C code

DISCA-C is the first code, which implements the intranuclear cascade evaporation model describing the interaction of particles with pre-formed clusters and their emission in nuclear reactions induced by projectiles of intermediate energy [49]. The code was used for the calculation of energy and angular distributions of α-particles, the (p, xnypzα) reaction cross-sections and other applications. The brief description of the model is given in [50,51].

In the model the nucleus is broken up into 10 concentric zones with uniform density. The radius of the outermost zone is estimated by the condition that the nucleon density in this region being 0.01 of that in the nucleus center. The nuclear density for medium and heavy nuclei ($A > 16$) is estimated by Woods-Saxon function. The momentum distribution for nucleons for each zone is defined according to Fermi gas model. It is supposed that besides of nucleons the nucleus consists of "pre-formed" clusters tritons, ^{3}He nuclei and α-particles. The deuteron clusters are not considered. Maximum kinetic energy of clusters, i.e. the Fermi energy, and their potentials are defined by following relations:

$$T_{\alpha,i}^F = 4T_{n,i}^F, \quad T_{t,i}^F = T_{h,i}^F = 3T_{n,i}^F, \tag{23}$$

$$\begin{aligned} &U_{\alpha,i} = T_{n,i}^F + Q_\alpha, \quad U_{t,i} = T_{t,i}^F + Q_t, \\ &U_{h,i} = T_{h,i}^F + Q_h, \end{aligned} \tag{24}$$

where $T_{n,i}^F$ is the Fermi energy for nucleon in ith nuclear zone; $T_{t,i}^F$, $T_{h,i}^F$ and $T_{\alpha,i}^F$ are the Fermi energy for tritons, ^{3}He and α-particles, respectively; Q_z is the separation energy calculated from the experimental nuclide masses, z = t, ^{3}He and α; $U_{z,i}$ is the nuclear potential for each type of particles. According to [52] the momentum distributions for tritons, ^{3}He and α-particles are taken as

$$N_t(\mathbf{p}_t)d\mathbf{p}_t = N_h(\mathbf{p}_h)d\mathbf{p}_h \propto p^6\,dp\,d\Omega \tag{25}$$

and

$$N_\alpha(\mathbf{p}_\alpha)d\mathbf{p}_\alpha \propto p^8\,dp\,d\Omega. \tag{26}$$

The definition of the point of the intranuclear interaction and partner characteristics is discussed in detail in [50].

For a nucleon "x" moving inside the nucleus with the kinetic energy T, the probability of the interaction with nuclear matter is calculated as follows:

$$\begin{aligned} Q_i = \rho_i(&\varphi_n\sigma^{xn}(T) + \varphi_p\sigma^{xp}(T) + \varphi_\alpha\sigma^{x\alpha}(T) \\ &+ \sigma_{p\text{-}u}^x(T)), \end{aligned} \tag{27}$$

where ρ_i is the nucleon density in the ith zone; σ^{xn} and σ^{xp} are cross-sections for the interactions with intranuclear neutron and proton, correspondingly; $\sigma^{x\alpha}$ is the cross-section for interaction with pre-formed α-cluster; $\sigma^{x}_{p\text{-}u}$ is the cross-section for the pick-up process combining the nucleon of x-type and pre-formed triton or ^{3}He cluster to form an α-particle; φ_n, φ_p and φ_α are relative numbers of neutrons, protons and α-clusters in the nucleus. A value of φ_α adopted in the present work is equal to 0.05. Values φ_n and φ_p are calculated from the total number of nucleons and the φ_α value.

For excited α-particles, the elastic scattering and break-up processes in the interactions with intranuclear nucleons are considered. The approximations from [53,50] are used for calculating the nucleon–nucleon and nucleon–α-particle interaction cross-sections. The energy dependence of the pick-up cross-section $\sigma^{x}_{p\text{-}u}(T)$ is defined according to the form-factor $F_{1,3}$ calculated in [44], which corresponds to the formation of the α-particle from three nucleons with energy below the Fermi energy and one nucleon with energy above the Fermi energy. The cross-section is equal to

$$\sigma^{x}_{p\text{-}u}(T) = \varsigma(-1.011\times10^{-6}\varepsilon^3 + 1.748\times10^{-4}\varepsilon^2 - 1.128\times10^{-2}\varepsilon + 0.275742)/(R\rho_i), \quad (28)$$

where $\varepsilon = T - T^{F}_{n,i}$ $(\varepsilon < 67)$; $R = 1.25A^{1/3}$; ζ is the fitting parameter equal to 14 in the present work. The angular distribution for nucleon–nucleon and nucleon–α-particle scattering is calculated with the help of the formulas from [51,54,50].

The reflection and refraction of particle momenta on the nuclear zone boundaries is considered. The Pauli principle is taken into account as for nucleon–nucleon, as for nucleon–α-collisions. In an addition, the restriction on the orbital momenta of nucleons after the interaction [55] is considered. According to [56] the orbital momenta l of nucleons colliding within the square potential well should not exceed the product of asymptotic nucleon momentum and the nucleus radius: $l \leqslant p_a R$, where p_a is the linear momentum the nucleon would have outside the nucleus, R is the nucleus radius. This restriction on l results from the fact that the nucleus has no states below the centrifugal barrier [56]. For a multi-zone nuclear density model, the restriction on the orbital momenta of nucleons colliding in the ith zone has the form

$$l_i \leqslant p_{i+1}R_i, \quad (29)$$

where l_i is the orbital momentum of the nucleon with momentum p_i in the ith zone; p_{i+1} is the momentum the nucleon would have in the $i+1$th zone (the zones are numbered beginning from the nucleus center); R_i is the radius of the ith zone in which the two nucleons collide.

The restriction on the orbital momenta, superimposed by Eq. (29), reduces the total number of intranuclear interactions, which results to an increase in the emission of high energy particles from the nucleus [55,56]. The calculations show [55] that use of Eq. (29) along with the Pauli principle and with the consideration of the reflection/refraction effects on nuclear zone boundaries improves substantially the agreement with experimental data at low and intermediate energies of primary particles.

The majority of computer codes based on the intranuclear cascade evaporation model, e.g. the codes included in the MCNPX package [57] (Section 2.3), disregard condition Eq. (29). To some extent the effect can be compensated by the neglect the refraction and reflection of the particle momentum at the boundary of nuclear zones (default MCNPX option). However, such neglect is not physically well founded [56].

The equilibrium particle emission is described by the Weisskopf–Ewing model [22]. The nuclear level density is calculated according to the Fermi gas model

$$\rho(U) = (1/12)\pi^{1/2}a^{-1/4}U^{-5/4}\exp(2\sqrt{aU}) \quad (30)$$

at the high excitation energy U and by the "constant temperature" model at low energy of excitation. The value of the nuclear level density parameter is taken equal to $A/9$. The inverse reaction cross-sections are calculated according to phenomenological formulas from [58] approximating the results of optical model calculations.

Evaporation is considered for neutrons, protons, deuterons, tritons, ^{3}He nuclei and α-particles.

2.2.2. The DISCA-S code

DISCA-S is the simplified version of the DISCA code. The simulation of processes involving α-clusters is not performed. The model used for the description of nucleon–nucleon interactions is discussed in [51,59,55]. The code was successfully used for the calculation of activation and transmutation cross-sections [60,61], atomic displacement cross-sections [62], complex particle production cross-sections [63,64], energy and angular distributions of nucleons [55,59].

The yield of composite particles emitted during the cascade stage of reaction is described by the nuclear bond breakdown approach [65]. According to [65] the fragment "x" formation cross-section is equal to

$$\sigma_x^{\mathrm{casc}}(E_p) = \sigma_{\mathrm{non}}(E_p) N_0 (A/A_x)(N_{\mathrm{casc}}/A)^{m_0 \varepsilon}, \qquad (31)$$

where $\sigma_{\mathrm{non}}(E_p)$ is the non-elastic cross-section for the interaction of the primary particle with kinetic energy E_p and a nucleus; A_x is mass number of the fragment; A is the mass number of target nucleus; N_{casc} is the average number of nucleons emitted from nucleus on the cascade stage of the reaction; $\varepsilon = Q_x + V_x$, where Q_x is the separation energy for the fragment in the nucleus; V_x is the Coulomb potential for the fragment; N_0 and m_0 are parameters. The values of parameters obtained in [63] for the α-particle emission are used in the present work, $N_0 = 0.12$ and $m_0 = 0.06$. The Coulomb potential V_x is calculated as $0.21Z + 2.5$ MeV, where Z is atomic number of the target nucleus.

The nuclear density distribution is calculated as in the DISCA-C code. The Pauli principle and the restriction on the orbital momenta, Eq. (29) are checked for each intranuclear interaction. The refraction and reflection of nucleon momentum are considered at the nuclear zone boundaries.

The nuclear level density for equilibrium states is calculated with the approximate formula $\rho(U) = C\exp(2\sqrt{aU})$, where $a = A/9$. The inverse reaction cross-section for neutrons is calculated according to [66]. The "sharp cut-off" formulas from [23] are used for the calculation of the inverse reaction cross-sections for charged particles.

2.3. Intranuclear cascade model combined with pre-equilibrium exciton model and evaporation model

This section makes an outline of nuclear models used in the MCNPX code package [57] for the description of the particle interactions with nuclei. Four intranuclear cascade models are implemented in MCNPX: Bertini [67,68], ISABEL [53,69,70], CEM2k [71,51,72–75] and INCL4 [76,77]. Except INCL4, the models are combined with the pre-equilibrium exciton model and with the evaporation model. Namely first three models (Bertini, ISABEL and CEM2k) describe fast complex particles emission with the help of the exciton model. The approach [78] proposed for the light cluster emission description by authors of the INCL4 model is not implemented in MCNPX yet. It is not discussed here, although the INCL4 model combined with the evaporation model is used for the comparison with the experimental data in Section 3.

2.3.1. The Bertini and ISABEL modules of MCNPX

The common feature of the Bertini model [67,68] and the ISABEL model [53,69,70] is the approximation of the real nuclear density distribution by concentric zones with constant density. The ISABEL model implies the division of the nucleus in sixteen zones and the Bertini model presents three-zone division [79]. The main difference between all models consists in the approaches used for the intranuclear interaction simulation, determination of the point of particle interaction, selection of collision partners for the moving nucleons and pions and the parameterization of n–n and π–n cross-sections. The brief overview of the models is given in [80].

As typical intranuclear cascade models, Bertini and ISABEL underestimate the angular distribution of secondary nucleons at high emission angles [81]. The necessity to solve this problem by the consideration of the nucleon and pre-formed cluster interactions was mentioned 30 years ago [82]. It is not done yet. To improve the agreement between calculations and experimental data the pre-equilibrium exciton model algorithm [83,79] has been

added to intranuclear cascade models. The basic expressions for the calculation of pre-equilibrium particle emission spectra have been obtained from the analytical solution of master equations describing the evolution of excited nucleus. The pre-equilibrium emission rate for the α-particle leaving the exciton state (p, h) with the excitation energy E is calculated as follows [83]:

$$W_\alpha(\varepsilon_\alpha, p, h, E) = \frac{(2S_\alpha + 1)\mu_\alpha \varepsilon_\alpha \sigma_\alpha(\varepsilon_\alpha)}{\pi^2 \hbar^3} \times \frac{\omega(p-4, h, E - Q_\alpha - \varepsilon_\alpha)}{\omega(p, h, E)} F_\alpha, \tag{32}$$

where the factor F_α defines the probability of the α-particle formation.

Eq. (32) relates to the first pre-equilibrium model for complex particle emission formulated by Kalbach–Cline [84]. The model has been analyzed and criticized in [85]. From the formal point of view, the consideration of the final nuclear state corresponding to the α-emission as with the $n-4$ excitons and the use of the energy independent α-formation probability factor result in too low emission rates for α-particles comparing with experimental data [85].

The equilibrium particle emission is described by the Dresner approach [86] and by the advanced ABLA model [87]. They are used in a various combination with the Bertini and ISABEL intranuclear cascade models. Dresner and ABLA implement different models for the nuclear level density calculation. Both models are based on the simplified approaches for the calculation of particle emission widths and inverse reaction cross-sections. Simplifications are made to get analytical expressions for the widths avoiding the integration of emission rates during the simulation of the particle evaporation cascade. Their justifications can be made from the thorough comparison of results of the calculation with experimental data.

In the calculations discussed below intranuclear cascade models are always used together with the pre-equilibrium and evaporation models. An indication on the cascade model "Bertini" and "ISABEL" implies also the application of the pre-compound exciton algorithm describing the de-excitation of residual nuclei formed after the fast particle emission.

The present calculations are based on the default set of input parameters of the models, which are described in [57,88].

2.3.2. The CEM2k module MCNPX

The Cascade Exciton Model (CEM) implemented in the MCNPX package has being developed and improved during last three decades [71,51,72–75]. It was a first model [72] combining the intranuclear cascade evaporation model and the pre-equilibrium exciton model. Later such combination was applied for many codes [49].

The nuclear density distribution is approximated in CEM by the step function with seven nuclear regions of the uniform density. The refraction and reflection effects for nucleon momentum are not considered as in calculations with the Bertini and ISABEL models using the default set of the input MCNPX parameters. New approximation for elementary cross-sections is used for the intranuclear event simulation. Many refinements and improvements of the model including the description of momentum-energy conservation on the cascade stage of reaction and new systematics for the level density parameters are discussed in [75].

The pre-equilibrium exciton model employed after the simulation of the cascade stage of reaction is described in [72,49]. The pre-equilibrium emission rate for α-particles is calculated according to the "coalescence" model proposed by Ribansky and Oblozinsky [85]

$$W_\alpha(\varepsilon_\alpha, p, h, E) = \frac{(2S_\alpha + 1)\mu_\alpha \varepsilon_\alpha \sigma_\alpha(\varepsilon_\alpha)}{\pi^2 \hbar^3} \gamma_\alpha \frac{\omega(4, 0, \varepsilon_\alpha + Q_\alpha)}{g_\alpha} \times \frac{\omega(p-4, h, E - Q_\alpha - \varepsilon_\alpha)}{\omega(p, h, E)} R_\alpha, \tag{33}$$

where γ_α is the formation probability for the α-particle; R_α is the factor providing the correct combination of protons and neutrons to form outgoing α-particle [85]. The values of γ_α and R_α are evaluated theoretically. The approach [85] is analyzed in [44].

2.4. Systematics

Systematics is a useful tool for the evaluation of nuclear reaction cross-sections in case experimental data are absent and theoretical calculations are not reliable. A set of systematics is used in the present work for the evaluation of α-particle production cross-section for proton and neutron induced reactions.

2.4.1. Proton induced reactions

The α-particle production cross-section is evaluated at the primary proton energies equal to 18, 62, 90, 160 and 600 MeV as follows:

$$E_p = 18\ \text{MeV}, \quad Z \geqslant 60,$$
$$\sigma_\alpha = \pi r_0^2 (A^{1/3}+1)^2 A^{-5.42} (-4991 \cdot P + 2252)^3, \tag{34}$$

$$E_p = 62\ \text{MeV}, \quad Z \geqslant 6,$$
$$\sigma_\alpha = 183.05 \exp(-7.578 \cdot R)\ \text{mb}, \tag{35}$$

$$E_p = 90\ \text{MeV}, \quad Z \geqslant 13,$$
$$\sigma_\alpha = 245.85 \exp(-4.9572 \cdot R)\ \text{mb}, \tag{36}$$

$$E_p = 160\ \text{MeV}, \quad Z \geqslant 12,$$
$$\sigma_\alpha = 226.7 \exp(-0.01047 \cdot Z)\ \text{mb}, \tag{37}$$

$$E_p = 600\ \text{MeV}, \quad Z \geqslant 26,$$
$$\sigma_\alpha = 537 \cdot Z^{-0.102}\ \text{mb}, \tag{38}$$

where Z and A are the atomic number and the atomic mass number of target nucleus; $r_0 = 1.3$ fm; $P = (A - 2 \cdot Z + 0.5)/A$; $R = (A - 2Z)/A$. Eq. (34) refers to the (p, α) cross-section rather than to the α-particle production cross-section. Eqs. (37) and (38) were obtained for natural mixtures of isotopes.

Eq. (34) was obtained using the (p, α) cross-section for five nuclei from ^{150}Nd to ^{176}Yb measured at 18 MeV and for ^{197}Au measured at 18.4 MeV in [89]. The cross-section for ^{197}Au at 18 MeV was estimated basing on the excitation function for the (p, α) reaction calculated by GNASH and fitted to the measured cross-section at 18.4 MeV. Eqs. (35) and (36) have been obtained in [14] with the help of experimental data from [90] for eight nuclei from ^{12}C to ^{209}Bi at 62 MeV, and from [91] for four nuclei from ^{27}Al to ^{209}Bi at 90 MeV. The systematics at 160 MeV (Eq. (37)) was produced using the measured cross-sections for Mg, Al and Si from [92], for Fe from [93,94], for Ni from the compilation [51], for Ag, Au and Bi from [95] and for Th from [96,97]. Data from [98], which seem incomplete, were not included in the analysis. The necessary interpolation and extrapolation of data from [92,51] for Mg, Al, Si and Ni were done to get the cross-section values at the proton energy 160 MeV. The α-particle production cross-sections measured in [99,100] for Fe, Ni, Ag, Pb and Bi were used to derive Eq. (38). The cross-section for Cu at 600 MeV equal to 575 mb [51] essentially different with other measurements [99,100] was not included in the analysis.

One should note that Eqs. (34)–(38) have been obtained using a few numbers of experimental points. These formulas can be used only for a crude estimation of α-particle production cross-section.

2.4.2. Neutron induced reactions

A theoretical formula for the evaluation of the (n, α) reaction cross-section has been derived in [101,102] using basic expressions for the particle emission spectrum of the pre-equilibrium exciton and evaporation models. The parameters of the formula were obtained from the fitting to the (n, α) reaction cross-sections measured for 120 nuclei with $A \geqslant 39$ at the neutron energy of 14.5 MeV [101]. The formula is $E_n = 14.5$ MeV, $18 \leqslant Z \leqslant 50$,

$$\sigma(n,\alpha) = \pi r_0^2 (A^{1/3}+1)^2 \exp(-209.11 \cdot S^2 + 8.4723 \cdot P - 0.19253 \cdot Z/A^{1/3} - 0.96249), \tag{39a}$$

$Z > 50$

$$\sigma(n,\alpha) = \pi r_0^2 (A^{1/3}+1)^2 (-1.6462 \cdot P + 0.39951)^3, \tag{39b}$$

where Z and A are the atomic number and the atomic mass number of target nucleus; $r_0 = 1.3$ fm; $P = (A - 2 \cdot Z + 0.5)/A$, $S = (A - 2Z + 1)/A$.

At the neutron energy of 20 MeV the parameter values of the systematics for the (n, α) reaction cross-section have been obtained using the results of theoretical calculations [102] $E_n = 20$ MeV,

$18 \leqslant Z \leqslant 50$,

$$\sigma(n,\alpha) = \pi r_0^2 (A^{1/3}+1)^2 \exp(-37.317 \cdot S^2 - 7.2027 \cdot P - 0.22669 \cdot Z/A^{1/3} - 2.027), \quad (40a)$$

$Z > 50$,

$$\sigma(n,\alpha) = \pi r_0^2 (A^{1/3}+1)^2 (-0.86267 \cdot P + 0.26976)^3. \quad (40b)$$

Eqs. (39) and (40) are used in the present work for the (n, α) reaction cross-section evaluation.

2.5. Nonelastic interaction cross-sections

To exclude the difference in the calculated α-particle production cross-sections caused by the use of different reaction cross-sections (σ_{non}) the calculations with the help of the GNASH, ALICE/ASH, DISCA and MCNPX codes were performed with the same non-elastic reaction cross-section for a certain nucleus under investigation. The adopted σ_{non} values were taken from ENDF/B-VI, calculated with the help of the optical model with the potential from [17] or obtained from the MCNPX calculations.

3. Comparison of calculations with experimental data

The available experimental data for ^{197}Au give detail information about the total and differential cross-sections for the α-particle production. These data are used for the comparison with results of the calculation.

3.1. Energy distribution of α-particles emitted

The experimental energy distribution of emitted α-particles is an information, which is suitable for comprehensive test of nuclear models describing the complex particle emission.

Fig. 1 shows the α-particle emission spectra for p+^{197}Au reaction measured in [103,104] and calculated with the help of the GNASH code and by the ALICE/ASH code at the primary proton energy 72.3 and 200 MeV. Experimental double differential cross-sections for the α-particle emission for the reaction induced by the 200 MeV protons [104] were angle integrated to get the energy distribution. The calculation of the α-particle emission spectra was done with the help of different models for the nuclear level density calculation [10–12].

Rather good agreement is observed between the pre-equilibrium α-spectrum calculated with the

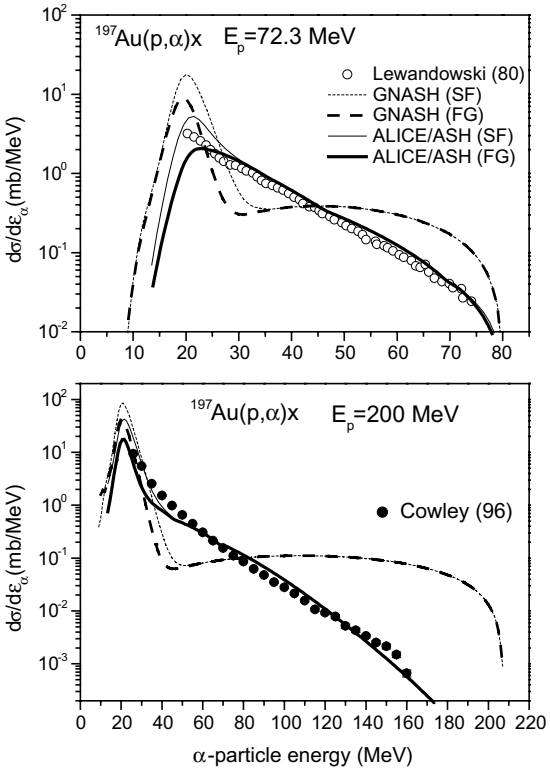

Fig. 1. The α-particle emission spectra for p+^{197}Au reaction induced by protons with the energy 72.3 and 200 MeV calculated with the help of the GNASH code and the ALICE/ASH code using different models for the description of the nuclear level density: the Fermi gas model [10] (FG) and the generalized superfluid model (SF). The measured data are from [103,104].

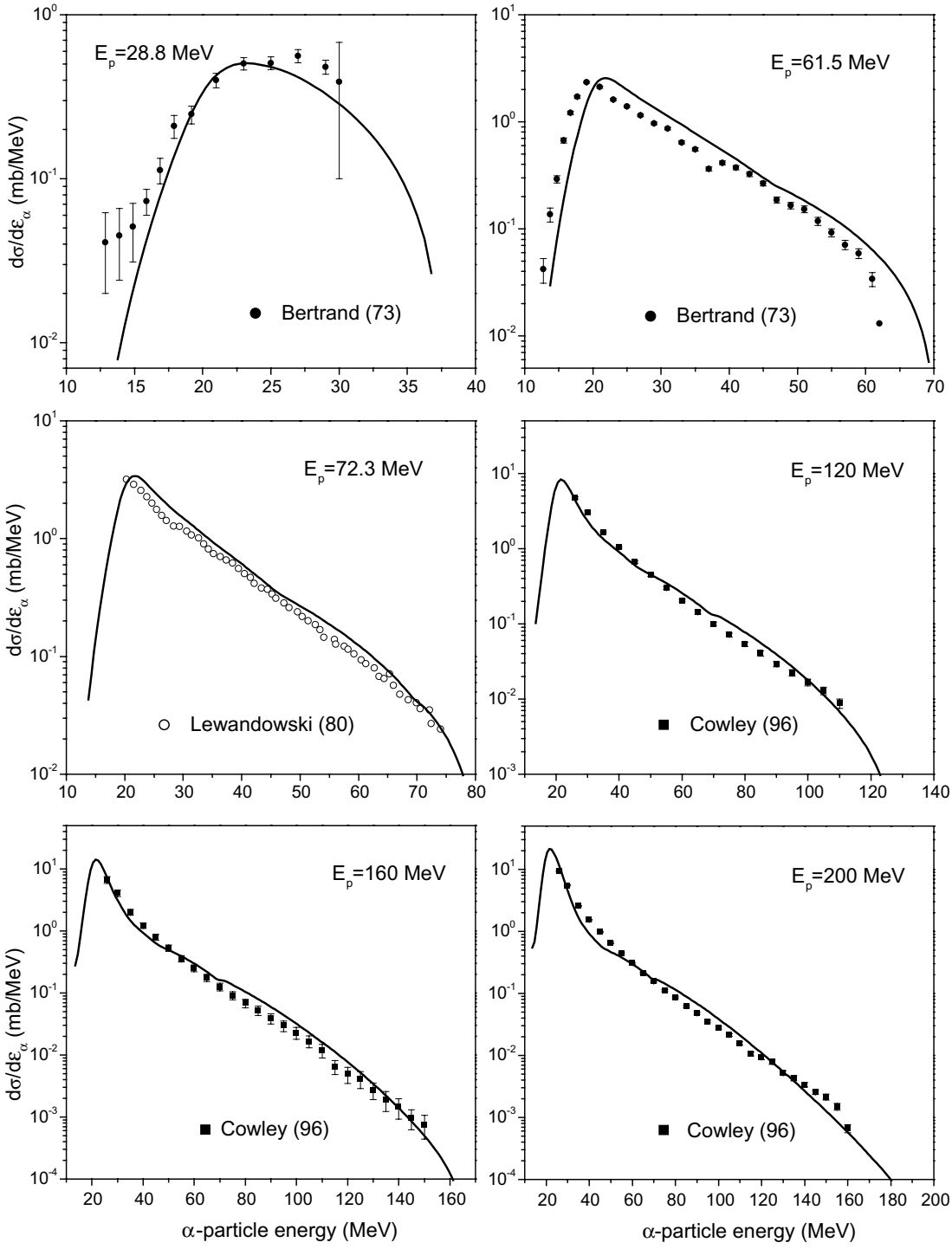

Fig. 2. The α-particle emission spectra calculated with the help of the ALICE/ASH code for p+^{197}Au reaction at the primary proton energies from 28.8 to 200 MeV. The nuclear level density parameter "*a*" is equal to *A*/13. The experimental data are from [90,103,104].

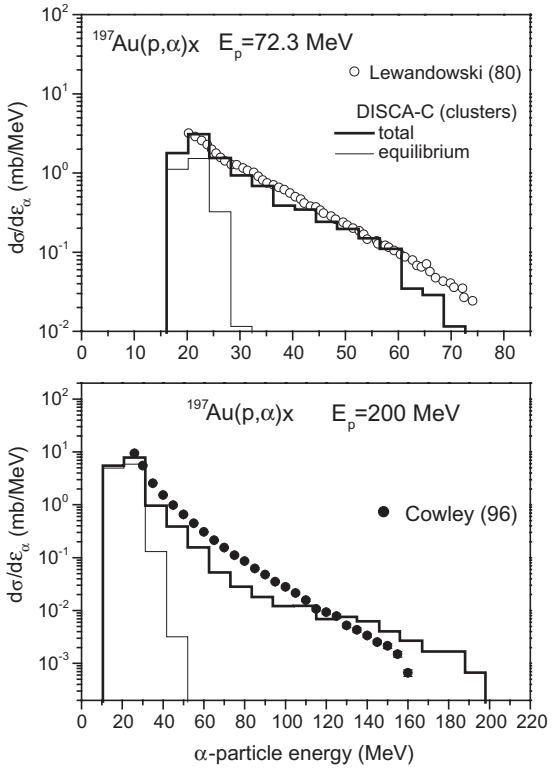

Fig. 3. The α-particle emission spectra for p+^{197}Au reaction induced by protons with the energy 72.3 and 200 MeV calculated with the help of the DISCA-C code. The measured data are from [103,104].

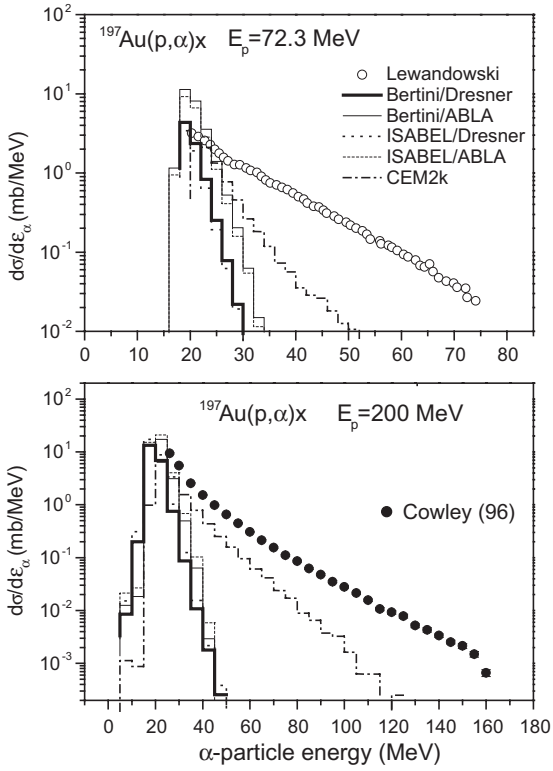

Fig. 4. The α-particle emission spectra for p+^{197}Au reaction induced by protons with the energy 72.3 and 200 MeV calculated by MCNPX with the help of different models: Bertini/Dresner, Bertini/ABLA, ISABEL/Dresner, ISABEL/ABLA and CEM2k. The measured data are from [103,104].

help of the ALICE/ASH code and experimental data. The GNASH code underestimates the α-particle emission spectrum at the energies after the evaporation peak and strongly overestimates the spectrum at high emission energies. The use of different models for nuclear level density calculation results in a considerable difference in the description of the evaporation spectrum. The calculation with the help of GNASH and ALICE/ASH using the superfluid nuclear model overestimates the equilibrium part of the spectrum comparing with experimental data. Most probably, it is caused by the lack of nuclear level density parameters derived from experimental data and by the use of global systematics to get the parameter values for many residual nuclei. The use of the Fermi gas model [10] results in too much low values of the evaporation spectrum (upper Fig. 1) calculated by the ALICE/ASH code.

A reasonable description of the measured evaporation peak in the α-particle spectrum and the experimental total α-particle yield (Section 3.3) for the p+^{197}Au reaction is obtained using the simple model for nuclear level density calculation based on the use of Eq. (30) with the nuclear level density parameter equal to $A/13$. The example of such calculation of α-particle emission spectra performed with the help of the ALICE/ASH code is shown in Fig. 2 for proton induced reactions at primary energies from 28.8 to 200 MeV. The use of this approach cannot be considered as a consistent solution of the problem of the agreement of calculations and experimental data. It is used only for evaluation purposes.

Fig. 3 shows α-particle emission spectra from the p+^{197}Au reaction obtained by the simulation of nucleon and pre-formed nuclear clusters interactions with the help of the intranuclear cascade evaporation model implemented in the DISCA-C code. The contribution of the equilibrium α-emission is shown. It is seen that the main mechanism of the α-particle production at the ejectile energy above 30 MeV is the non-equilibrium emission. In whole, there is a satisfactory agreement between the result of calculations performed by the DISCA-C code and experimental spectra.

The α-particle spectra calculated with the help of different codes from the MCNPX package [57] are shown in Fig. 4. The calculation was done with the help of the Bertini model and the ISABEL model combined with the Multistage Pre-equilibrium Model (MPM) [83] and with the Dresner and ABLA evaporation models. Also, the CEM2k model implemented the intranuclear cascade, pre-equilibrium and evaporation model was used for the α-emission spectrum calculation. The agreement between calculations and experimental data [103,104] is quite poor. The α-particle spectrum calculated by the CEM2k model is the most close to experimental data. The Bertini and ISABEL models in different combinations with the Dresner and ABLA evaporation models describe only the evaporation range of the α-particle emission spectra. The application of the MPM pre-equilibrium exciton model [83] coupling with Bertini and ISABEL does not substantially improve the agreement with experimental data comparing with the pre-equilibrium model [72] implemented in CEM2k. One should note that the use of the ABLA model comparing with the Dresner model overestimates the α-particle equilibrium spectrum (upper Fig. 4). This fact is important for the further analyses of the difference between calculated and experimental yields of α-particles in nuclear reactions discussed in Section 3.3.

3.2. Non-equilibrium α-particle yield

The contribution of the non-equilibrium emission in the total α-particle yield have been obtained from the analyses of experimental data for ^{197}Au irradiated with protons in [95,97,105–107].

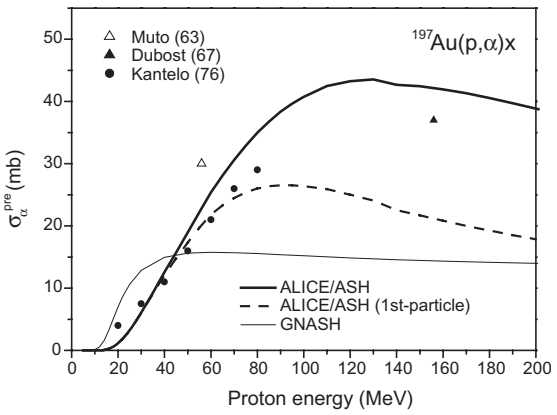

Fig. 5. The non-equilibrium component of the α-particle production cross-section for p+^{197}Au reaction calculated with the help of the GNASH code and the ALICE/ASH code. The measured data are from [95,106,107].

According to [107] the contribution of the non-equilibrium α-particle emission in the total α-particle production decreases from 100% at the primary proton energy 20 MeV to 73% at 40 MeV and to 60% at 80 MeV. At the proton energy 156 MeV the contribution of the non-equilibrium α-particle yield is about 33% [95].

Fig. 5 shows the non-equilibrium component of the α-particle production cross-section (σ_α^{pre}) calculated with the help of the GNASH code and the ALICE/ASH code. The contribution of the first pre-compound α-particle obtained by ALICE/ASH is also shown. The reasonable agreement is observed between the data and the ALICE/ASH code calculations. The calculated σ_α^{pre} cross-section passes through a maximum at 130 MeV and slowly decreases with the primary proton energy growing. Probably, the decrease of the σ_α^{pre} value results because the escape of the third and subsequent pre-compound α-particles is not taken into account (Section 2.1.2).

Results obtained with the help of different intranuclear cascade models are shown in Fig. 6. The pre-compound α-particle emission is described by exciton models in all cases except the use of the DISCA-C and DISCA-S codes. The cross-sections σ_α^{pre} calculated using the Bertini and ISABEL models are too low comparing with data [95,106,107]. The DISCA-C code gives the reasonable description of experimental data. DISCA-S better repro-

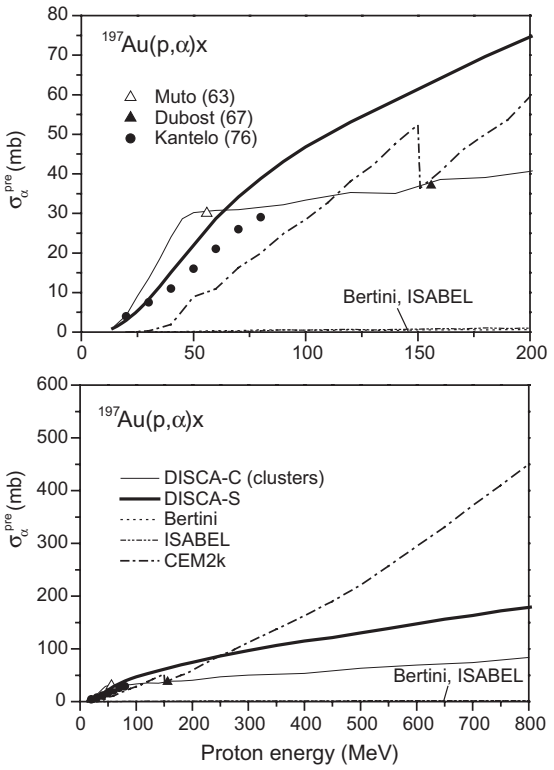

Fig. 6. The non-equilibrium component of the α-particle production cross-section for p+^{197}Au reaction calculated with the help of the DISCA-C and DISCS-S codes and calculated by MCNPX using the Bertini, ISABEL and CEM2k models. The measured data are from [95,106,107].

duces experimental σ_α^{pre} values [106,107] below 80 MeV. The agreement with the data [95] at 156 MeV can be improved by the appropriate choice of model parameters, Eq. (31).

The CEM2k model reproduces the general trend of the σ_α^{pre} cross-section below 80 MeV. The calculated cross-section has a jump near 150 MeV, whose origin is not clear. The same jump is observed in the displacement cross-section calculated by CEM2k in [81]. The inconsistency of the calculation at 150 MeV should be removed in future versions of the MCNPX code.

At the energies above 400 MeV the difference between different calculations is rather big (lower Fig. 6). The new measurements, which would make it possible to extract and to analyze the pre-equilibrium component of the α-particle production cross-section, are necessary in order to answer a question about the advantages of different methods of the α-particle cross-section calculation at these energies.

3.3. Total α-particle production

The α-particle production cross-section (σ_α) for proton induced reactions on ^{197}Au calculated by different codes is compared with experimental data in Figs. 7–10.

Fig. 7 shows measured α-production cross-sections [89,90,95,97,106–108], results of calculations performed with the help of the GNASH and ALICE/ASH codes and the systematics values, Eqs. (34)–(37). The calculations were carried out using different approaches for the description of the nuclear level density [10–12,23,30]. The difference between the σ_α cross-section calculated by the same code and with the help of various models describing the level density is observed above 40 MeV. It is in a general agreement with a fact that the pre-equilibrium emission is the main origin of α-particles produced in the proton irradiation of ^{197}Au at the energies below 40 MeV. The good agreement is observed between the experimental data, systematics and the σ_α values calculated by the ALICE/ASH code using the superfluid nuclear model [12] and the Fermi gas

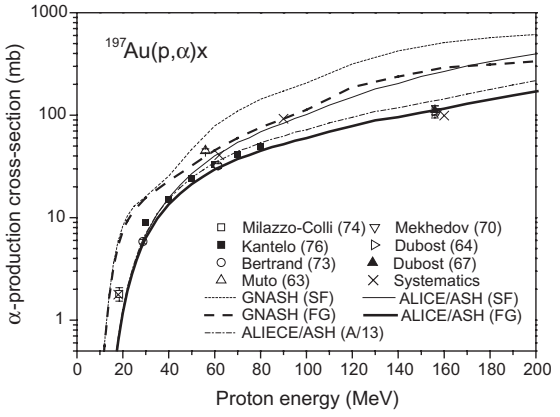

Fig. 7. The α-particle production cross-section for the proton irradiation of ^{197}Au at the energy up to 200 MeV calculated with the help of the GNASH and ALICE/ASH codes, estimated by systematics and measured in [89,90,95,97,106–108].

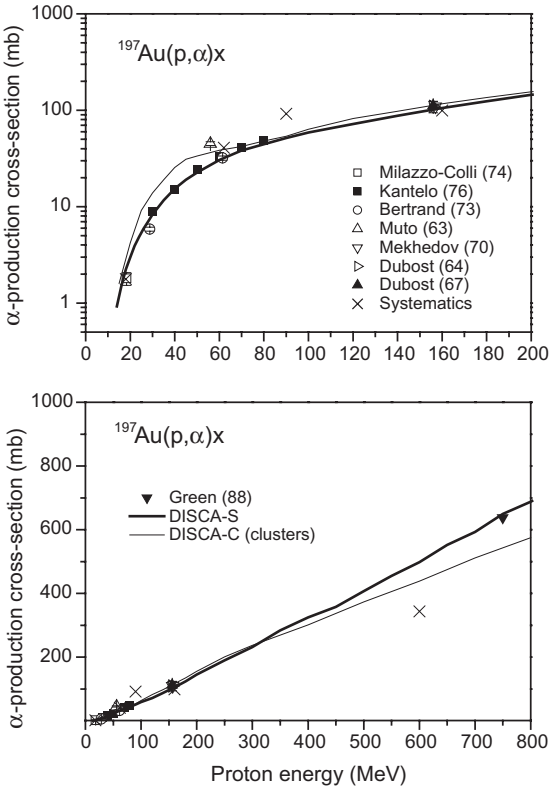

Fig. 8. The α-particle production cross-section for the proton irradiation of ^{197}Au calculated with the help of the DISCA-C and DISCA-S codes, estimated by systematics and measured in [89,90,95,97,106–109].

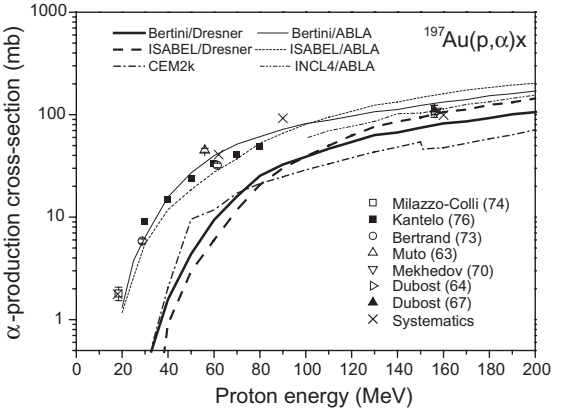

Fig. 9. The α-particle production cross-section for the proton irradiation of ^{197}Au at the energy below 200 MeV calculated with the help of the Bertini/Dresner, Bertini/ABLA, ISABEL/Dresner, ISABEL/ABLA, INCL4/ABLA and CEM2k models, estimated by systematics and measured in [89,90,95,97,106–108].

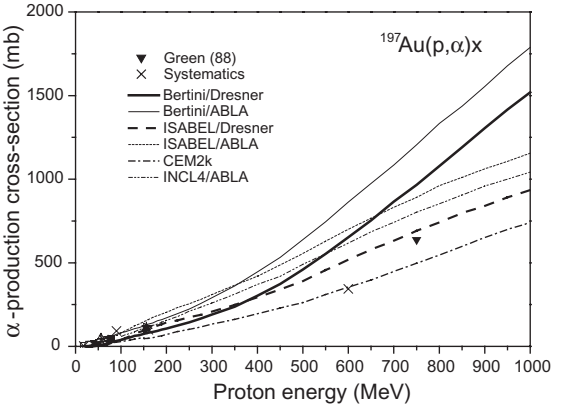

Fig. 10. The α-particle production cross-section for the proton irradiation of ^{197}Au at the energy up to 1 GeV calculated with the help of the Bertini/Dresner, Bertini/ABLA, ISABEL/Dresner, ISABEL/ABLA, INCL4/ABLA and CEM2k models, estimated by systematics and measured in [89,90,95,97,106–109].

model [10] at the primary proton energies below 90 MeV. At the energy around 150 MeV the α-particle production cross-section calculated using the Fermi gas model [10] is in a better agreement with the available experimental data than the σ_α values obtained with the help of the superfluid model. The acceptable agreement is observed between the experimental data and the σ_α values calculated by the ALICE/ASH code using the Fermi gas model with the nuclear level density parameter equal to $A/13$. The α-particle production cross-section calculated by the GNASH code is rather higher than the experimental points.

All models implemented in GNASH and ALICE/ASH overestimate the σ_α cross-sections at the energies above 200 MeV comparing with calculations carried out by the DISCA-C and DISCA-S codes and the codes from the MCNPX package. In particular the calculated contribution of the equilibrium α-particle emission in the total production cross-section is too big. The main reason is that the energy of 200 MeV is likely out of the range of the applicability of pre-equilibrium models implemented in GNASH and ALICE/

ASH. The limitation results from the approximate description of the nuclear geometry, the calculation of the *R*-factors (Eqs. (1) and (15)), the description of multiple pre-compound nucleon emission and others having impact on the calculated distribution of the excitation energy available for the particle evaporation.

Fig. 8 shows the total α-particle production cross-section calculated with the help of the DISCA-C code and the DISCA-S code. The σ_α values calculated with the help of the DISCA-C code are in the general agreement with experimental data. At the same time the calculated α-production cross-section is higher than experimental points at the energies below 60 MeV and lower than the measured σ_α value [109] at 750 MeV. There is an excellent agreement between the α-production cross-section calculated by the DISCA-S code and measured cross-sections in a whole energy range from 18 to 750 MeV, where experimental data are available.

The α-particle production cross-section obtained with the help of codes from the MCNPX package is shown in Figs. 9 and 10. The detail view for the proton energies below 200 MeV is given in Fig. 9. The σ_α values calculated using the Bertini/ABLA and ISABEL/ABLA models are in the agreement with experimental data below the proton energy 150 MeV. At the same time, there is a discrepancy between the σ_α values calculated by the Bertini/Dresner and ISABEL/Dresner models and experimental cross-sections at these energies. At first sight the use of the ABLA model improves the agreement of calculations with measured data. On the other hand this improvement is obtained by the increased evaporation component of the σ_α cross-section, because the contribution of the non-equilibrium α-particle emission in σ_α predicted by the Bertini and ISABEL models is negligible (Section 3.2). As a consequence the use of the ABLA model results in a poor agreement with experimental data at high proton energies (Fig. 10). The best result for the combination of ABLA with intranuclear cascade model is observed for the INCL4/ABLA calculations. One should note that this result is observed for INCL4, where the simulation of the non-equilibrium α-particle emission is not performed.

The best agreement is observed between the experimental cross-section at 750 MeV [109] and calculations performed with the help of the ISABEL/Dresner model (Fig. 10). The cross-section calculated by the CEM2k model is in the agreement with the systematics value at 600 MeV.

The comparison of the results of calculations with experimental data discussed in this section shows that the reasonable evaluation of the α-particle production cross-section can be performed using the ALICE/ASH code, the DISCA-C or DISCA-S codes. The calculation by the ISABEL/Dresner model is also of interest at the energies above 150 MeV.

4. Evaluation of α-particle production cross-section

The evaluation of the α-particle production cross-section was done using the results of model calculations, systematics predictions and available experimental data. Calculations were performed by the ALICE/ASH code, the DISCA-S code and the ISABEL and Dresner modules of the MCNPX package.

4.1. ^{181}Ta

4.1.1. Proton induced reactions

Fig. 11 shows the α-particle production cross-section for ^{181}Ta irradiated with protons calculated by the ALICE/ASH code, the DISCA-S code and the ISABEL/Dresner (MCNPX) code. The detail view of the energy range below 200 MeV, which corresponds to the rapid change in the cross-section value, is given in upper Fig. 11. The σ_α values obtained by systematics Eqs. (34)–(38), the α-production cross-section measured [106] at the proton energy 56 MeV and the cross-section obtained from the analyses of the experimental data [95,110] at 156 and 800 MeV are also shown in Fig. 11. To get the total α-particle production cross-section at 156 MeV the measured yield [95] of α-particles having isotropic angular distribution (100 mb) was added by the value obtained in [95] for heavy nuclei relating to anisotropic α-particle emission (37 mb). The helium production

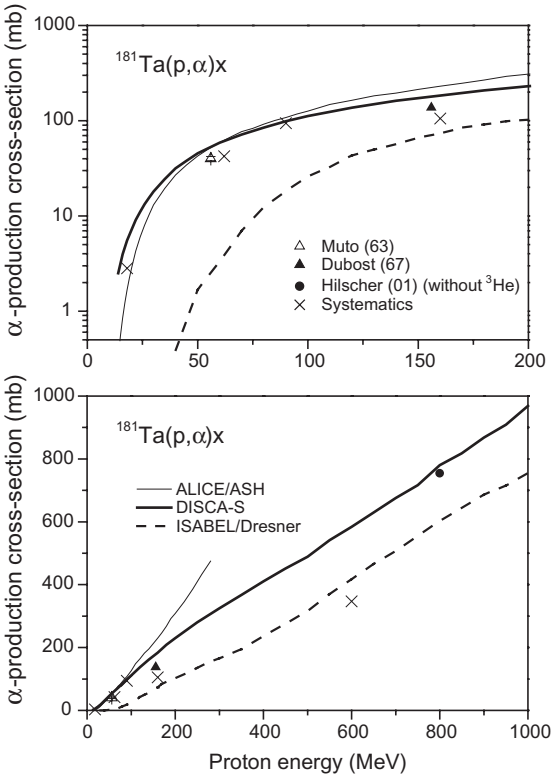

Fig. 11. The α-particle production cross-section for proton irradiation of ^{181}Ta calculated by the ALICE/ASH code, the DISCA-S code and the ISABEL/Dresner (MCNPX) code, estimated by systematics, measured in [106] and extracted from experimental data [95,110].

cross-section measured [110] at 800 MeV was corrected to exclude the contribution of ^{3}He. The yield of ^{3}He was estimated using the ^{3}He- and ^{4}He-production cross-section measured for seven elements from Al to Au in [109] at the proton energy 750 MeV and using experimental yields of ^{3}He and ^{4}He obtained in [111] for Au at 1.8 GeV. Fig. 11 shows a reasonable agreement between the σ_α cross-sections calculated by the ALICE/ASH and DISCA-S codes and experimental data and systematics values.

The results of calculations, systematics values and available measured data were assumed as the basis for the evaluation of the α-particle production cross-section for ^{181}Ta. The evaluated data are shown in Fig. 12 and Table 1.

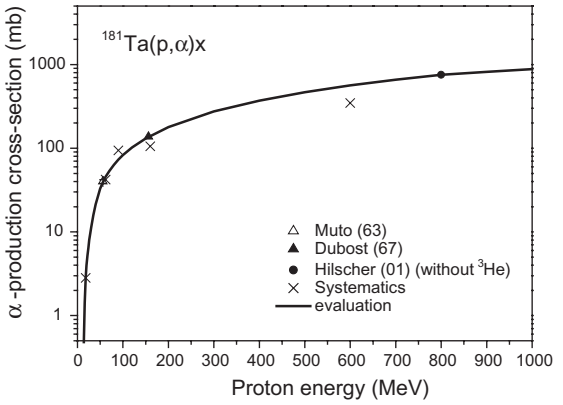

Fig. 12. The evaluated α-particle production cross-section for ^{181}Ta irradiated with protons.

4.1.2. Neutron induced reactions

Experimental data for neutron induced reactions on ^{181}Ta are available at the energies below 20 MeV. Except the measurement of the α-production cross-section in [112] other data [113–120] were obtained for (n, α) reaction. The data measured recently [117–120] were not taken into account in the most of the evaluation for national and international data files.

A new evaluation of the α-particle production cross-section was performed for ^{181}Ta in the present work. The cross-sections were obtained separately for the reactions ^{181}Ta(n, α)^{178g}Lu and ^{181}Ta(n, α)^{178m}Lu ($T_{1/2}$ = 23.1 min) using measured data from [115,117–120].

The sum of cross-sections obtained for reactions producing ^{178g}Lu and ^{178m}Lu, available experimental data, systematics values and the data from FENDL/A-2, JENDL-3.3, CENDL-2 and JEFF-3/A [121] are shown in Fig. 13.

The total α-particle production cross-section at the energies below 20 MeV was obtained using the cross-section evaluated for the (n, α) reaction and the data for the (n, nα) reaction taken from JEFF-3/A (data are from the ADL-3 library [122]).

At the energies above 20 MeV the α-particle production cross-section has been calculated with the help of theoretical models. The evaluated α-particle production cross-section for ^{181}Ta irradiated with neutrons at the energies up to 1 GeV is shown in Fig. 14 and Table 2.

Table 1
The evaluated ^{4}He production cross-section from ^{181}Ta, ^{nat}W and ^{197}Au irradiated with protons at the energies up to 1 GeV

Proton energy[a] (MeV)	^{4}He production cross-section (mb)		
	^{181}Ta	^{nat}W	^{197}Au
6	4.15×10^{-6}	2.26×10^{-4}	1.21×10^{-3}
8	6.84×10^{-4}	1.86×10^{-3}	7.95×10^{-3}
10	1.70×10^{-2}	1.43×10^{-2}	4.47×10^{-2}
12	0.135	8.848×10^{-2}	0.201
14	0.548	0.391	0.599
16	1.42	1.20	1.22
18	2.82	2.57	1.87
20	3.98	4.18	2.62
22	5.22	5.92	3.47
24	6.50	7.22	4.39
26	8.00	8.63	5.39
28	9.46	10.2	6.46
30	11.3	11.9	7.67
35	15.8	16.0	11.3
40	21.4	20.7	15.0
50	32.9	29.8	24.0
60	43.9	39.6	31.0
70	53.6	49.0	41.0
80	63.3	59.0	49.0
90	73.0	69.3	57.3
100	82.7	79.2	65.6
120	102	99.6	82.2
150	131	131	107
200	179	186	151
300	275	286	240
400	371	376	328
500	467	465	417
600	563	559	505
700	659	658	594
800	755	762	697
900	817	853	814
1000	880	920	932

[a] The cross-sections between the energy points shown should be found by the log–log interpolation of the data at the energies below 20 MeV, and by the linear–linear interpolation at the energies above 20 MeV.

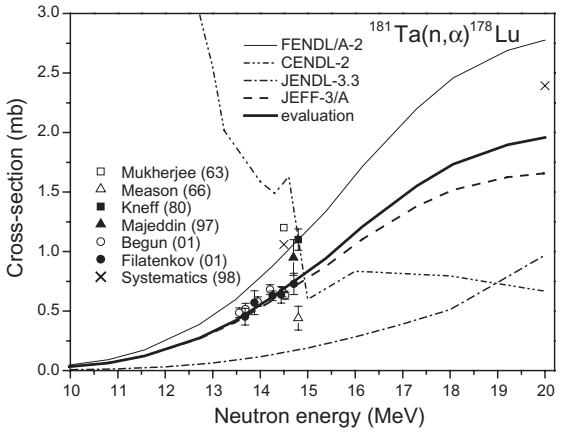

Fig. 13. The (n, α) reaction cross-section for ^{181}Ta taken from FENDL/A-2, JENDL-3.3, CENDL-2 and JEFF-3/A, measured in [112–120], estimated by systematics and evaluated in the present work.

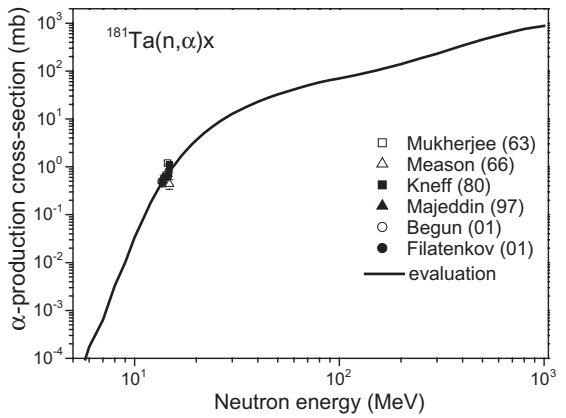

Fig. 14. The evaluated α-particle production cross-section for ^{181}Ta irradiated with neutrons.

4.2. ^{nat}W

To obtain the cross-sections for natural tungsten the calculations were performed for tungsten isotopes ^{180}W, ^{182}W, ^{183}W, ^{184}W and ^{186}W.

4.2.1. Proton induced reactions

Fig. 15 shows the α-particle production cross-section calculated by the ALICE/ASH code, the DISCA-S code and the ISABEL/Dresner (MCNPX) code, systematics values obtained at 18, 62, 90, 160 and 600 MeV and experimental data [109]. The data taken from ENDF/B-VI Proton Sublibrary (Release 7) and from JENDL-HE [123] are also shown. There is the good agreement between the σ_α cross-sections calculated with the help of the DISCA-S code and the experimental data [109] at 750 MeV. Data from JENDL-HE are in the agreement with systematics values at 62 and 90 MeV and with the cross-section calculated by ALICE/ASH at the energies from 100 to 150 MeV. As whole, the data from JENDL-HE and ENDF/B-VI differ substantially.

Table 2
The evaluated ^{4}He production cross-section from ^{181}Ta, ^{nat}W and ^{197}Au irradiated with neutrons at the energies from 5 MeV[a] up to 1 GeV

Neutron energy (MeV)	^{4}He production cross-section (mb)		
	^{181}Ta	^{nat}W	^{197}Au
5	1.49×10^{-5}	2.88×10^{-3}	4.00×10^{-7}
6	1.73×10^{-4}	5.31×10^{-3}	4.00×10^{-7}
7	6.27×10^{-4}	1.11×10^{-2}	4.00×10^{-7}
8[b]	3.26×10^{-3}	2.44×10^{-2}	2.40×10^{-2}
9	1.00×10^{-2}	5.62×10^{-2}	4.81×10^{-2}
10	3.36×10^{-2}	0.126	7.21×10^{-2}
11	8.00×10^{-2}	0.287	9.62×10^{-2}
12	0.182	0.572	0.120
13	0.335	0.922	0.156
14	0.570	1.32	0.301
14.5	0.719	1.53	0.439
15	0.868	1.74	0.577
16	1.23	2.23	1.00
17	1.71	2.74	1.47
18	2.28	3.20	1.86
19	2.91	3.72	2.21
20	3.61	4.37	2.52
22	5.17	5.47	3.65
24	6.91	7.24	4.96
26	8.78	9.14	6.40
28	10.7	11.1	7.92
30	12.7	13.3	9.48
35	17.7	18.5	13.6
40	22.8	23.0	17.9
45	27.9	27.5	21.3
50	32.4	30.9	25.0
60	41.3	37.3	29.0
70	49.9	44.2	35.0
80	57.9	51.5	41.1
90	64.5	57.9	46.2
100	70.3	64.8	50.9
120	82.2	77.8	63.2
150	102	99.3	78.7
200	139	139	111
250	185	181	151
300	231	229	191
400	340	344	300
500	452	449	403
600	556	552	499
700	656	655	591
800	753	760	696
900	817	852	814
1000	879	920	931

[a] Data below 5 MeV can be found in JEFF-3/A [121].
[b] For ^{197}Au the cross-section is equal to 4.0×10^{-07} mb [121] at the energy from 7 to 8 MeV.

The evaluation of the α-particle production cross-section was based on the results of the ALICE/ASH and DISCA codes calculations and the systematics value at 18 MeV. The evaluated cross-section is shown in Table 1 and Fig. 16.

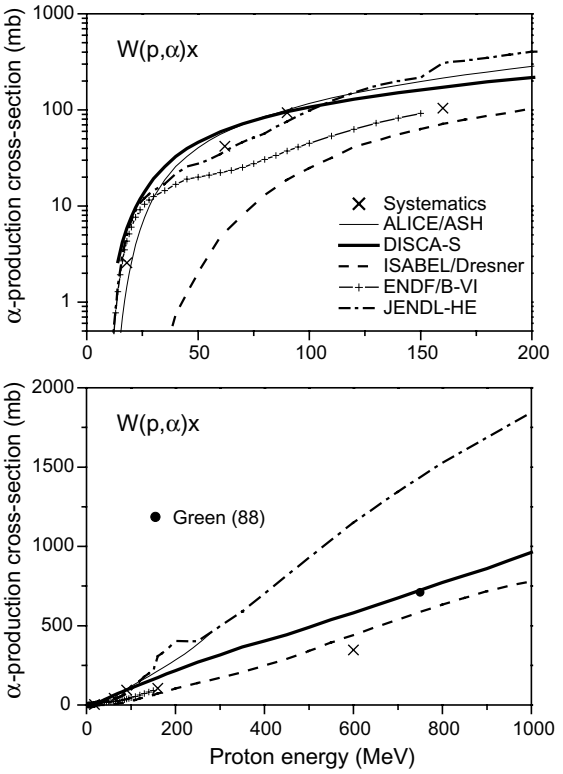

Fig. 15. The α-particle production cross-section for proton irradiation of natural tungsten calculated by the ALICE/ASH code, the DISCA-S code and the ISABEL/Dresner (MCNPX) code, estimated by systematics, taken from ENDF/B-VI and JENDL-HE and measured in [109].

4.2.2. Neutron induced reactions

To get the α-particle production cross-section for natural tungsten the data for isotopes ^{180}W, ^{182}W and ^{183}W were taken from JEFF-3/A at the energies below 20 MeV. The new evaluation was performed for the (n, α) reaction cross-section for ^{184}W and ^{186}W. For both isotopes the JENDL-3.3 data were fitted to the cross-section measured in [115,124,125] for ^{184}W and in [115,124–127] for ^{186}W. The (n, nα) reaction cross-section was taken from JEFF-3/A. The data obtained for natural tungsten were adjusted to the results of calculations at the energies above 20 MeV.

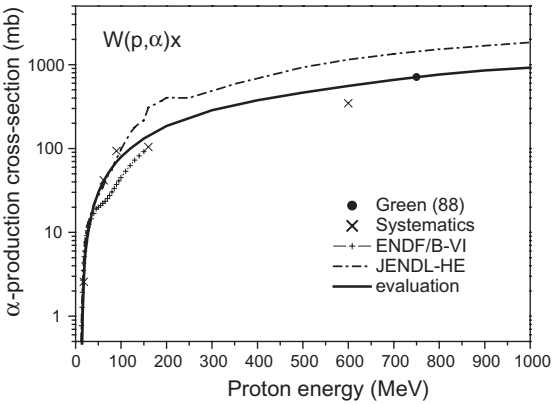

Fig. 16. The α-particle production cross-section for tungsten irradiated with protons evaluated in the present work and taken from ENDF/B-VI and JENDL-HE.

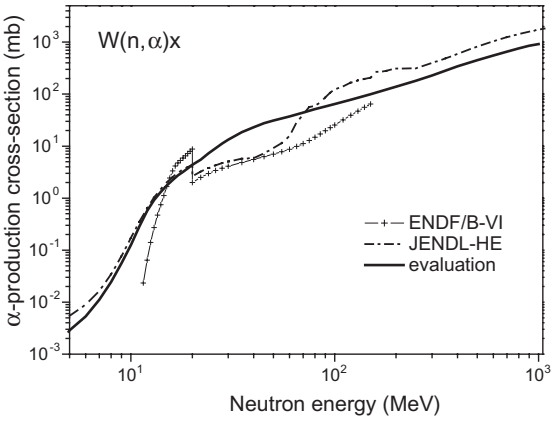

Fig. 17. The α-particle production cross-section for tungsten irradiated with neutrons evaluated in the present work and taken from ENDF/B-VI and JENDL-HE.

Evaluated σ_α values are shown in Fig. 17 and Table 2. For the comparison data from ENDF/B-VI and JENDL-HE are also plotted in Fig. 17.

4.3. ^{197}Au

4.3.1. Proton induced reactions

The comparison of the α-particle production cross-section calculated using different nuclear models with experimental data for ^{197}Au is discussed in detail in Section 3. The data evaluated in the present work are shown in Fig. 18 and Table 1.

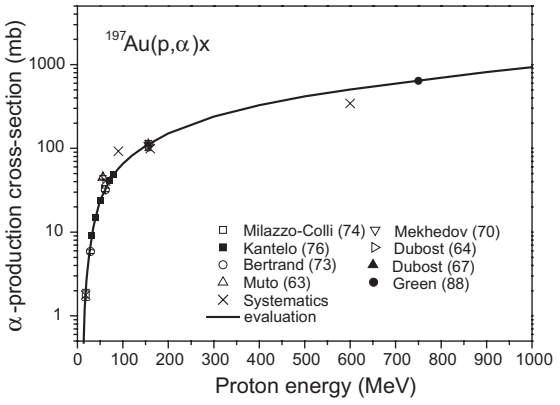

Fig. 18. The evaluated α-particle production cross-section for ^{197}Au irradiated with protons.

4.3.2. Neutron induced reactions

Data from JEFF-3/A for (n, α) reaction were adopted after the comparison with experimental data [112,125,128] at the energy below 15 MeV. At the energies from 15 to 20 MeV the (n, α) cross-section is taken from ENDF/B-VI. The data for (n, nα) reaction were taken from JEFF-3/A. The calculation of the α-particle production cross-section was performed with the help of the ALICE/ASH code and the DISCA-S code at the energy above 20 MeV. The evaluated cross-section is shown in Fig. 19 and Table 2.

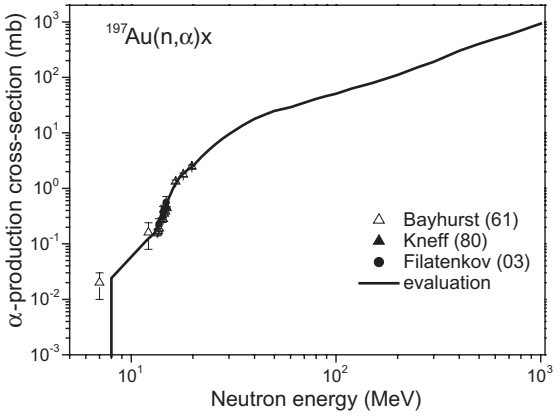

Fig. 19. The evaluated α-particle production cross-section for ^{197}Au irradiated with neutrons.

5. Conclusion

Different approaches and models used for the description of the α-particle emission in the reactions induced by intermediate energy nucleons on ^{181}Ta, tungsten isotopes and ^{197}Au were discussed. The comparison of the results of calculations with experimental data shows

(i) The pre-equilibrium exciton model implemented in the GNASH code gives a crude description of the α-particle spectra (Fig. 1). Calculations underestimate the α-spectrum at the energies after the evaporation peak and give too high spectrum values at high emission energies. The calculated pre-equilibrium yield of α-particles σ_{α}^{pre} is too low comparing with the data obtained from the analyses of experiments. Partly, it results that the multiple pre-compound α-particle emission is not taken into account.

(ii) The Bertini model and the ISABEL model combined with the MPM exciton model [83] considerably underestimate the yield of non-equilibrium α-particles (Fig. 6). The CEM2k model describes the general energy dependence of the σ_{α}^{pre} cross-section at the energies below 80 MeV. There is a strong difference between the σ_{α}^{pre} values calculated by CEM2k and by other codes at the energy above 400 MeV. There is a discrepancy between α-particle emission spectra calculated by the codes from the MCNPX package and experimental data (Fig. 4).

(iii) The use of the ABLA evaporation model coupled with the Bertini, ISABEL and INCL4 models overestimates the contribution of the equilibrium α-particle emission in the α-spectra and the total α-particle production cross-section (Figs. 4 and 10).

(iv) The α-particle emission spectra, the non-equilibrium and the total α-particle yields calculated by the ALICE/ASH code and the DISCA-C and DISCA-S codes are in a reasonable agreement with experimental data (Figs. 1–3, 5–8).

The discrepancy between the results of calculations performed with the help of the codes from MCNPX and experimental data results from the use in the MPM and MEM exciton models [88] the early versions of the coalescence model describing the pre-compound α-particle emission [84,85]. It seems reasonable to implement in the GNASH code and the codes from MCNPX the models used for the description of the pre-equilibrium α-particle emission in the ALICE/ASH and DISCA-C codes.

In the present work the α-particle production cross-section has been evaluated for ^{181}Ta, natural tungsten and ^{197}Au at the energies of incident neutrons and protons from several MeV to 1 GeV. The evaluated cross-sections are shown in Table 1 and Figs. 12, 16, 18 for proton induced reactions and in Table 2 and Figs. 14, 17, and 19 for neutron induced reactions.

References

[1] C. Rubbia et al., in: Proc. Accelerator Applications in a Nuclear Renaissance (AccApp'03), San Diego, CA, 1–5 June 2003.
[2] W. Hauser, H. Feshbach, Phys. Rev. 87 (1952) 366.
[3] P.G. Young, E.D. Arthur, M.B. Chadwick, in: Proc. Int. Atomic Energy Agency Workshop on Nuclear Reaction Data and Nuclear Reactors, 15 April–17 May 1996, Vol. 1, p. 227;
Report LA-12343-MS (1992); GNASH-FKK: Pre-equilibrium, Statistical Nuclear-Model Code System for Calculation of Cross Sections and Emission Spectra, RSIC Code Package PSR-125.
[4] F.C. Williams, Nucl. Phys. A 166 (1971) 231.
[5] C. Kalbach, Z. Phys. A 287 (1978) 319.
[6] C. Kalbach, Z. Phys. A 283 (1977) 401.
[7] M.B. Chadwick, P.G. Young, D.C. George, Y. Watanabe, Phys. Rev. C 50 (1994) 996.
[8] A.Yu. Konobeyev, T. Fukahori, O. Iwamoto, Nuclear data evaluation for ^{238}Pu, ^{239}Pu, ^{240}Pu, ^{241}Pu and ^{242}Pu irradiated by neutrons and protons at the energies up to 250 MeV, Report JAERI-Research 2002-029, December 2002.
[9] M.B. Chadwick, P.G. Young, P. Oblozinsky, A. Marcinkowski, Phys. Rev. C 49 (1994) R2885.
[10] A.V. Ignatyuk, G.N. Smirenkin, A.S. Tishin, Sov. J. Nucl. Phys. 21 (1975) 255.
[11] A.V. Ignatyuk, Level Densities, in: Handbook for Calculations of Nuclear Reaction Data, Report IAEA-TEC-DOC-1034, 1998, p. 65. Available from: <http://www.nds.iaea.or.at/ripl/ripl_handbook.htm>.

[12] A.V. Ignatyuk, K.K. Istekov, G.N. Smirenkin, Yad. Fiz. 29 (1979) 875.
[13] G. Hansen, A. Jensen, Nucl. Phys. A 406 (1983) 236.
[14] A.Yu. Konobeyev, T. Fukahori, O. Iwamoto, Neutron and proton nuclear data evaluation for ^{235}U and ^{238}U at energies up to 250 MeV, Report JAERI-Research 2002-028, December 2002.
[15] Reference Input Parameter Library for Theoretical Calculations of Nuclear Reactions, Level Densities. File obninsk_bcs.dat, http://www.nds.iaea.or.at/ripl/densities.htm.
[16] A.Yu. Konobeyev, T. Fukahori, O. Iwamoto, Nuclear data evaluation for ^{237}Np, ^{241}Am, ^{242g}Am and ^{242m}Am irradiated by neutrons and protons at energies up to 250 MeV, Report JAERI-Research 2002-032, December 2002.
[17] A.J. Koning, J.P. Delaroche, Nucl. Phys. A 713 (2003) 231, data are taken from <http://ndswebserver.iaea.org/RIPL-2/>.
[18] V. Avrigeanu, P.E. Hodgson, M. Avrigeanu, Phys. Rev. C 49 (1994) 2136.
[19] J. Raynal, ECIS96, in: Proc. Specialists' Meeting on the Nucleon Nucleus Optical Model up to 200 MeV, Bruyères-le-Chatel, France, 13–15 November 1996. Available from: <http://www.nea.fr/html/science/om200/raynal.pdf>.
[20] M. Blann, Phys. Rev. Lett. 28 (1972) 757.
[21] M. Blann, H.K. Vonach, Phys. Rev. C 28 (1983) 1475.
[22] V.F. Weisskopf, D.H. Ewing, Phys. Rev. 57 (1940) 472.
[23] M. Blann, ALICE-91: Statistical Model Code System with Fission Competition, RSIC Code Package PSR-146.
[24] A.Yu. Konobeyev, Yu.A. Korovin, P.E. Pereslavtsev, Code ALICE/ASH for calculation of excitation functions, energy and angular distributions of emitted particles in nuclear reactions, Obninsk Institute of Nuclear Power Engineering, 1997.
[25] A.I. Dityuk, A.Yu. Konobeyev, V.P. Lunev, Yu.N. Shubin, New advanced version of computer code ALICE-IPPE, Report INDC(CCP)-410, 1998.
[26] A.Yu. Konobeyev, A.Yu. Korovin, Kerntechnik 59 (1994) 72.
[27] A.Yu. Konobeyev, V.P. Lunev, Yu.N. Shubin, Acta Phys. Slovaca 45 (1995) 705.
[28] A.Yu. Konobeyev, Yu.A. Korovin, Kerntechnik 61 (1996) 45.
[29] A.Yu. Konobeyev, Yu.A. Korovin, P.E. Pereslavtsev, Izvestija Vuzov. Ser.: Yadernaja Energetika (Transactions of High School. Ser.: Nuclear Power Engineering) 1 (1997) 2.
[30] Yu.N. Shubin, V.P. Lunev, A.Yu. Konobeyev, A.I. Dityuk, Cross-section library MENDL-2 to study activation and transmutation of materials irradiated by nucleons of intermediate energies, Report INDC(CCP)-385, 1995.
[31] A.Yu. Konobeyev, Yu.A. Korovin, M. Vecchi, Kerntechnik 64 (1999) 216.
[32] A.Yu. Konobeyev, Yu.A. Korovin, V.P. Lunev, V.S. Masterov, Yu.N. Shubin, Voprosy Atomnoi Nauki i Techniki (Problems of Nuclear Science and Technology), Series: Nuclear Data 3–4 (1992) 55.
[33] Yu.N. Shubin, V.P. Lunev, A.Yu. Konobeyev, A.I. Dityuk, MEND-2P. Proton reaction data library for nuclear activation, Report IAEA-NDS-204, 1998. Available from: <http://www.nds.iaea.org/reports/nds-204.pdf>.
[34] U. Fischer, D. Leichtle, A. Konobeyev, Yu. Korovin, U. von Möllendorff, P.E. Pereslavtsev, I. Schmuck, Intermediate energy activation file 2001 (IEAF-2001), Report of Forschungszentrum Karlsruhe, Interner Bericht, IRS-Nr.10/01-Fusion-Nr.179, August 2001.
[35] Yu.A. Korovin, A.Yu. Konobeyev, P.E. Pereslavtsev, A.Yu. Stankovsky, C. Broeders, I. Broeders, U. Fischer, U. von Möllendorf, Nucl. Instr. and Meth. A 463 (2001) 544.
[36] U. Fischer, A. Konobeyev, Yu. Korovin, D. Leichtle, U. Von Möllendorff, P.E. Pereslavtsev, I. Schmuck, S.P. Simakov, H. Tsige-Tamirat, P.P.H. Wilson, in: Proc. Workshop on Nuclear Data for the Transmutation of Nuclear Waste, GSI, Darmstadt, 1–5 September 2003. Available from: <http://www.wnt.gsi.de/tramu/proceedings/Fischer.pdf>.
[37] A.Yu. Konobeyev, Yu.A. Korovin, V.I. Plyaskin, Kerntechnik 59 (1994) 87.
[38] A.Yu. Konobeyev, Yu.A. Korovin, P.E. Pereslavtsev, V.I. Plyaskin, A.Yu. Stankovsky, WIND. Nuclear data library for transactinides at energies up to 100 MeV, Report INDC(CCP)-384, 1995.
[39] Yu.A. Korovin, A.Yu. Konobeyev, P.E. Pereslavtsev, V.I. Plyaskin, A.Yu. Stankovsky, Prog. Nucl. Ener. 29 (Suppl.) (1995) 297.
[40] E. Daum, U. Fischer, A.Yu. Konobeyev, Yu.A. Korovin, V.P. Lunev, U. von Möllendorff, P.E. Pereslavtsev, M. Sokcic-Kostic, A.Yu. Stankovsky, P.P.H. Wilson, D. Woll, Neutronics of the High flux test region of the international fusion materials irradiation facility (IFMIF), Report of Forschungszentrum Karlsruhe, FZKA 5868, June 1997.
[41] Yu.A. Korovin, A.Yu. Konobeyev, P.E. Pereslavtsev, A.Yu. Stankovsky, C. Broeders, I. Broeders, U. Fischer, U. von Möllendorff, P. Wilson, D. Woll, in: Proc. Int. Conf. Nuclear Data for Science and Technology, Trieste, Italy, May 1997, p. 851.
[42] A.Yu. Konobeyev, Yu.A. Korovin, Kerntechnik 60 (1995) 147.
[43] E. Betak, J. Dobes, Z. Phys. A 279 (1976) 319.
[44] A. Iwamoto, K. Harada, Phys. Rev. C 26 (1982) 1821.
[45] K. Sato, A. Iwamoto, K. Harada, Phys. Rev. C 28 (1983) 1527.
[46] P. Obložinský, I. Ribanský, Phys. Lett. B 74 (1978) 6.
[47] O.T. Grudzevich, A.V. Zelenetsky, A.B. Pashchenko, KOP code for calculation of cross-section for interaction of neutrons and charged particles with atomic nuclei

based on optical model, Report of Institute of Physics and Power Engineering, Obninsk, N1802, 1986.
[48] J.R. Huizenga, G. Igo, Nucl. Phys. 29 (1962) 462.
[49] International codes and model intercomparison for intermediate energy activation yields, NSC/DOC(97)-1, January 1997, <http://www.nea.fr/html/science/docs/1997/nsc-doc97-1/>.
[50] A.Yu. Konobeyev, Yu.A. Korovin, P.E. Pereslavtsev, U. Fischer, U. von Möllendorff, Nucl. Sci. Eng. 139 (2001) 1.
[51] V.S. Barashenkov, V.D. Toneev, Interaction of High Energy Particles and Atomic Nuclei with Nuclei, Atomizdat, Moscow, 1972.
[52] A. Ferrero, E. Gadioli, E. Gadioli Erba, I. Iori, N. Molho, L. Zetta, Z. Phys. A 293 (1979) 123.
[53] K. Chen, Z. Fraenkel, G. Friedlander, J.R. Grover, J.M. Miller, Y. Shimamoto, Phys. Rev. 166 (1968) 949.
[54] V.I. Ostroumov, R.A. Filov, Sov. Phys. JETP 37 (10) (1959) 459.
[55] A.Yu. Konobeyev, Yu.A. Korovin, Kerntechnik 63 (1998) 124.
[56] V.E. Bunakov, M.M. Nesterov, I.A. Tarasov, Bull. Acad. Sci. USSR Phys. Ser. 41 (10) (1977) 168;
V.E. Bunakov, M.M. Nesterov, I.A. Tarasov, Izv. Akad. Nauk SSSR Ser. Fiz. 41 (1977) 2187.
[57] J.S. Hendricks, G.W. Mckinney, L.S. Waters, T.L. Roberts, et al., MCNPX Extensions, Version 2.5.0, Report LA-UR-04-0570, February 2004.
[58] A. Chatterjee, K.H.N. Murthy, S.K. Gupta, Optical reaction cross sections for light projectiles, Report INDC(IND)-27/GJ, 1980.
[59] Yu.N. Shubin, V.P. Lunev, A.Yu. Konobeyev Yu.A. Korovin, in: Proc. of a Specialists Meeting. Intermediate Energy Nuclear Data: Models and Codes, Issy-Les-Moulineaux, France, 30 May–1 June 1994, p. 35. Available from: <http://www.nea.fr/html/science/docs/pubs/iendsm94/>.
[60] V.V. Artisyuk, A.Yu. Konobeyev, Yu.A. Korovin, Kerntechnik 58 (1993) 174.
[61] Yu.A. Korovin, A.Yu. Konobeyev, P.E. Pereslavtsev, in: Proc. Int. Conf. on Emerging Nuclear Energy Systems, Makuhari, Japan, September 1993, p. 444.
[62] A.Yu. Konobeyev, Yu.A. Korovin, V.N. Sosnin, J. Nucl. Mater. 186 (1992) 117.
[63] A.Yu. Konobeyev, Yu.A. Korovin, J. Nucl. Mater. 195 (1992) 286.
[64] A.Yu. Konobeyev, Yu.A. Korovin, Nucl. Instr. and Meth. B 82 (1993) 103.
[65] F.P. Denisov, V.N. Mekhedov, Nuclear Reactions at High Energies, Atomizdat, Moscow, 1972.
[66] I. Dostrovsky, Z. Fraenkel, G. Friedlander, Phys. Rev. 116 (1959) 683.
[67] H.W. Bertini, Phys. Rev. 131 (1963) 1801.
[68] H.W. Bertini, Phys. Rev. 188 (1969) 1711.
[69] Y. Yariv, Z. Fraenkel, Phys. Rev. C 20 (1979) 2227.
[70] Y. Yariv, Z. Fraenkel, Phys. Rev. C 24 (1981) 488.
[71] A.S. Iljinov, A code for intranuclear cascade calculation in the energy range <5 GeV, Report JINR B1-4-5478, Dubna, 1970.
[72] K.K. Gudima, S.G. Mashnik, V.D. Toneev, Nucl. Phys. A 401 (1983) 329.
[73] S.G. Mashnik, in: Proc. of a Specialists Meeting. Intermediate Energy Nuclear Data: Models and Codes, Issy-Les-Moulineaux, France, 30 May–1 June 1994, p. 107. Available from: <http://www.nea.fr/html/science/docs/pubs/iendsm94/>.
[74] S.G. Mashnik, A.J. Sierk, O. Bersillon, T. Gabriel, Nucl. Instr. and Meth. A 414 (1998) 68, Report LA-UR-97-2905 (1997), http://t2.lanl.gov/publications/publications.html.
[75] S.G. Mashnik, K.K. Gudima, I.V. Moskalenko, R.E. Prael, A.J. Sierk, Adv. Space Res. 34 (2004) 1288.
[76] J. Cugnon, C. Volant, S. Vuillier, Nucl. Phys. A 620 (1997) 475.
[77] A. Boudard, J. Cugnon, S. Leray, C. Volant, Phys. Rev. C 66 (2002) 044615.
[78] A. Boudard, J. Cugnon, S. Leray, C. Volant, Nucl. Phys. A 740 (2004) 195.
[79] L.S. Waters (Ed.), MCNPX^{TM} User's Manual, Version 2.3.0, Report LA-UR-02-2607, April 2002.
[80] K. Ackerstaff et al., Nucl. Instr. and Meth. A 491 (2002) 492.
[81] C.H.M. Broeders, A.Yu. Konobeyev, C. Villagrasa, J. Nucl. Mater. (2005) to be published.
[82] H.W. Bertini, G.D. Harp, F.E. Bertrand, Phys. Rev. C 10 (1974) 2472.
[83] R.E. Prael, M. Bozoian, Adaptation of the multistage preequilibrium model for the Monte Carlo method (I), Report LA-UR-88-3238, September 1988. Available from: <http://www.xdiv.lanl.gov/XCI/PEOPLE/rep/plist.html>.
[84] C.K. Cline, Nucl. Phys. A 193 (1972) 417.
[85] I. Ribanský, P. Obložinský, Phys. Lett. B 45 (1973) 318.
[86] L. Dresner, EVAP – A Fortran Program for calculating the evaporation of various particles from excited compound nuclei, Report ORNL-TM-196, 1961.
[87] A.R. Junghans, M. De Jong, H.-G. Clerc, A.V. Ignatyuk, G.A. Kudyaev, K.-H. Schmidt, Nucl. Phys. A 629 (1998) 635.
[88] MCNPX^{TM} User's Manual, Version 2.4.0, Report LA-CP-02-408, September 2002.
[89] L. Milazzo-Colli, G.M. Braga-Marcazzan, M. Milazzo, C. Signorini, Nucl. Phys. A 218 (1974) 274.
[90] F.E. Bertrand, R.W. Peelle, Phys. Rev. C 8 (1973) 1045.
[91] J.R. Wu, C.C. Chang, H.D. Holmgren, Phys. Rev. C 19 (1979) 698.
[92] I. Leya, H. Busemann, H. Baur, R. Wieler, M. Gloris, S. Neumann, R. Michel, F. Sudbrock, U. Herpers, Nucl. Instr. and Meth. B 145 (1998) 449.
[93] O.A. Schaeffer, J. Zähringer, Z. Naturforsch. A 13 (1958) 346.
[94] O.A. Schaeffer, J. Zähringer, Phys. Rev. 113 (1959) 674.
[95] H. Dubost, B. Gatty, M. Lefort, J. Peter, X. Tarrago, J. Phys. 28 (1967) 257.

[96] H. Gauvin, M. Lefort, X. Tarrago, Nucl. Phys. 39 (1962) 447.
[97] H. Dubost, M. Lefort, J. Peter, X. Tarrago, Phys. Rev. B 136 (1964) 1618.
[98] R.E. Segel, T. Chen, L.L. Rutledge Jr., J.V. Maher, J. Wiggins, P.P. Singh, P.T. Debevec, Phys. Rev. C 26 (1982) 2424.
[99] R. Michel, M. Gloris, H.-J. Lange, I. Leya, M. Luepke, U. Herpers, B. Dittrich-Hannen, R. Roesel, Th. Schiekel, D. Filges, P. Dragovitsch, M. Suter, H.-J. Hofmann, W. Woelfli, P.W. Kubik, H. Baur, R. Wieler, Nucl. Instr. and Meth. B 103 (1995) 183.
[100] K. Goebel, H. Schultes, J. Zähringer, Production cross sections of tritium and rare gases in various target elements, Report CERN 64-12, 1964, cited in [51].
[101] A.Yu. Konobeyev, V.P. Lunev, Yu.N. Shubin, Nucl. Instr. and Meth. B 108 (1996) 233.
[102] A.Yu. Konobeyev, Yu.A. Korovin, At. Energ. 85 (1998) 556.
[103] Z. Lewandowski, E. Loeffler, R. Wagner, H.H. Mueller, W. Reichart, P. Schober, E. Gadioli, E. Gadioli Erba, Lett. Nuovo Cimento 28 (1980) 15.
[104] A.A. Cowley, G.J. Arendse, J.W. Koen, W.A. Richter, J.A. Stander, G.F. Steyn, P. Demetriou, P.E. Hodgson, Y. Watanabe, Phys. Rev. C 54 (1996) 778.
[105] M. Lefort, J.P. Cohen, H. Dubost, X. Tarrago, Phys. Rev. B 139 (1965) 1500.
[106] J. Muto, H. Iton, K. Okano, N. Shiomi, K. Fukuda, Y. Omori, M. Kinara, Nucl. Phys. 47 (1963) 19.
[107] M.V. Kantelo, J.J. Hogan, Phys. Rev. C 13 (1976) 1095.
[108] B.N. Mekhedov, V.N. Mekhedov, 1970, cited by Ref. 51.
[109] S.L. Green, W.V. Green, F.H. Hegedus, M. Victoria, W.F. Sommer, B.M. Oliver, J. Nucl. Mater. 155/157 (1988) 1350.
[110] D. Hilscher, C.-M. Herbach, U. Jahnke, V. Tishchenko, M. Enke, D. Filges, F. Goldenbaum, R.-D. Neef, K. Nünighoff, N. Paul, H. Schaal, G. Sterzenbach, A. Letourneau, A. Böhm, J. Galin, B. Lott, A. Péghaire, L. Pienkowski, J. Nucl. Mater. 296 (2001) 83.
[111] M. Enke, C.-M. Herbach, D. Hilscher, U. Jahnke, O. Schapiro, A. Letourneau, J. Galin, F. Goldenbaum, B. Lott, A. Péghaire, D. Filges, R.-D. Neef, K. Nünighoff, N. Paul, H. Schaal, G. Sterzenbach, A. Tietze, L. Pienkowski, Nucl. Phys. A 657 (1999) 317.
[112] D.W. Kneff, B.M. Oliver, H. Farrar, L.R. Greenwood, in: Proc. Symp. on Neutron Cross Sections from 10 to 50 MeV, Brookhaven Nat. Lab., 12–14 May 1980, p. 289; D.W. Kneff, B.M. Oliver, H. Farrar, L.R. Greenwood, Nucl. Sci. Eng. 92 (1986) 491.
[113] S.K. Mukherjee, H.Bakhru, in: Proc. Symp. on Nuclear Physics and Solid State Physics, Bombay, India, 27 February–2 March 1963, p. 244.
[114] J.L. Meason, R. Ganapathy, P.K. Kuroda, Radiochim. Acta 6 (1966) 26.
[115] Y. Kasugai, H. Yamamoto, A. Takahashi, T. Iida, K. Kawade, Report JAERI-M-93-046, 1992, p. 277.
[116] A.D. Majeddin, V. Semkova, R. Doczi, Cs.M. Buczko, J. Csikai, Investigations on (n,alpha) cross sections in the 14 MeV region, EXFOR 31481, 1997.
[117] S.V. Begun, V.O. Zheltonozhskyj, I.M. Kadenko, V.K. Maidanyuk, V.M. Neplyuev, G.I. Primenko, L.V. Sadovnikov, V.K. Tarakanov, Zbirnik naukovyh prac Kyiv Inst. yadernyh doslidzhen 1 (1) (1999) 74.
[118] S.V. Begun, I.M. Kadenko, V.K. Maidanyuk, V.M. Neplyuev, V.A. Plujko, G.I. Primenko, V.K.Tarakanov, in: Proc. Features of Nuclear Excitation States and Mechanisms of Nuclear Reactions, 51th Meeting on Nuclear Spectroscopy and Nuclear Structure, Sarov, Russia, 3–8 September 2001, the Book of Abstracts, 2001, p. 203.
[119] S.V. Begun, I.M. Kadenko, V.K. Maidanyuk, V.M. Neplyuev, G.I. Primenko, V.K. Tarakanov, in: Proc. Int. Conf. on Nuclear Data for Science and Technology, Tsukuba, Ibaraki, Japan, 7–12 October 2001, Nuclear Science and Technology Supplement, 2 (1) (2002) 425.
[120] A.A. Filatenkov, S.V.Chuvaev, Measurement of a set of badly known neutron induced cross sections, RI-258, Khlopin Radiev. Inst., St. Petersburg, 2001.
[121] J.-Ch. Sublet, A.J. Koning, R.A. Forrest, J. Kopecky, The JEFF-3.0/A Neutron Activation File. EAF-2003 into ENDF-6 Format, JEFDOC-982, November 2003.
[122] O.T. Grudzevich, A.V. Zeleneckij, A.V. Ignatyuk, A.B. Pashchenko, Yadernye Konstanty 3–4 (1993) 1.
[123] JENDL High Energy Data File 2004, http://www.ndc.tokai.jaeri.go.jp/jendl/jendl.html#jendl-sp.
[124] A. Grallert, J. Csikai, Cs.M. Buczko, I. Shaddad, Investigations on the systematics in (n,alpha) cross sections at 14.6 MeV, Report INDC(NDS)-286, 131, 1993.
[125] A.A. Filatenkov, S.V.Chuvaev, Experimental determination of cross sections of a set of badly known neutron induced reactions for heavy elements (Z=74–79), Report RI-259, Khlopin Radiev. Inst., St. Petersburg, 2003.
[126] Y. Ikeda, C. Konno, K. Oishi, T. Nakamura, H. Miyade, K. Kawade, H. Yamamoto, T. Katoh, Activation cross section measurements for fusion reactor structural materials at neutron energy from 13.3 to 15.0 MeV using FNS facility, Report JAERI-1312, 1988.
[127] Kong Xiangzhong, Hu Shangbin, Yang Jingkang, Comm. Nucl. Data Prog. 17 (1997) 9.
[128] B.P. Bayhurst, R.J. Prestwood, J. Inorg. Nucl. Chem. 23 (1961) 173.